# DEVELOPMENT AND CHARACTERIZATION COLON-TARGETED ORAL DELIVERY SYSTEM OF CURCUMIN LOADED NANOSTRUCTURE LIPID CARRIER

JITTAKAN LERTPAIROD

A Thesis Submitted to the Graduate School of Naresuan University
in Partial Fulfillment of the Requirements
for the Master of Science in Pharmacology and Biomolecular Sciences
2022

# DEVELOPMENT AND CHARACTERIZATION COLON-TARGETED ORAL DELIVERY SYSTEM OF CURCUMIN LOADED NANOSTRUCTURE LIPID CARRIER

JITTAKAN LERTPAIROD

A Thesis Submitted to the Graduate School of Naresuan University
in Partial Fulfillment of the Requirements
for the Master of Science in Pharmacology and Biomolecular Sciences
2022

Thesis entitled "Development and characterization colon-targeted oral delivery system of curcumin loaded nanostructure lipid carrier
"

By Jittakan Lertpairod

has been approved by the Graduate School as partial fulfillment of the requirements for the Master of Science in Pharmacology and Biomolecular Sciences of Naresuan University

**Oral Defense Committee**

..... Chair
( Chirasak Kusonwiriyawong, Ph.D.)

..... Advisor
(Associate Professor Waree Tiyaboonchai, Ph.D.)

..... Internal Examiner
(Assistant Professor Pakawadee Sermsappasuk, Ph.D.)

..... Internal Examiner
(Associate Professor Nanteetip Limpeanchob, Ph.D.)

**Approved**

.....
(Associate Professor Krongkarn Chootip, Ph.D.)
Dean of the Graduate School

**Title** DEVELOPMENT AND CHARACTERIZATION COLON-TARGETED ORAL DELIVERY SYSTEM OF CURCUMIN LOADED NANOSTRUCTURE LIPID CARRIER

**Author** Jittakan Lertpairod

**Advisor** Associate Professor Waree Tiyaboonchai, Ph.D.

**Academic Paper** M.S. Thesis in Pharmacology and Biomolecular Sciences, Naresuan University, 2022

**Keywords** Curcumin, Nanostructured lipid carrier (NLCs), pH-sensitive polymer, Inflammatory bowel disease, Colon, Bead

## ABSTRACT

This study aimed to develop an orally colon-targeted drug delivery system using a combination system of NLCs entrapped in pH-sensitive beads. Curcumin was used as a model drug. Curcumin-loaded NLCs, prepared by a hot-melt microemulsion method, manifested a mean size of 227.75±0.71 nm with a surface charge of -55.96±1.88 mV. A high entrapment efficiency of > 90% was observed. Subsequently, the curcumin-NLCs were entrapped in pH-sensitive beads, EudragitS100 (ES), using an ionotropic gelation method. The mean size of the curcumin-NLCs bead was 1 mm, with high curcumin entrapment efficiency of > 80%. The beads, observed by scanning electron microscope, illustrated a smooth densely packed structure in which curcumin-NLCs were evenly embedded in the polymer matrix. The in vitro drug release was accomplished under conditions mimicking stomach to colon transition. The results confirmed that the developed system could prevent drug release in the stomach. In addition, a sustained released behavior up to 12 h was observed in the

intestine and colon. The release kinetics was fitted with zero-order with a release mechanism followed an Hopfenberg, indicating the drug was released through polymer erosion at a constant rate. In conclusion, this research revealed that the developed pH-sensitive bead containing drug-loaded NLCs is a promising carrier for delivering drugs to the colon by oral administration.

# ACKNOWLEDGEMENTS

Foremost, I would like to express my sincere gratitude to my advisor, Assoc. Prof. Waree Tiyaboonchai for the continuous support of my study and research, for her patience, motivation, enthusiasm, and immense knowledge. Her guidance helped me all the time in my research. I could not have imagined having a better advisor and mentor for my research.

Besides my advisor, I would like to thank the rest of my thesis committee: Assoc. Prof. Nanteetip Limpeanchob, Asst. Prof. Pakawadee Sermsappasuk and Dr. Chirasak Kusonwiriyawong, for their encouragement, insightful comments, and challenging questions.

My sincere thanks also went to my labmates in the pharmaceutical technology unit, especially the RICOLA JUNGJING group, for the intensive discussions and suggestions to me about sample investigation. We were always discussed together even during tough or peak times, and for all the fun we have had in these last years.

Last but not least, I would like to thank my family: my parents, for giving birth to me in the first place and supporting me spiritually throughout my life.

Jittakan Lertpairod

# TABLE OF CONTENTS

**Page**

# LIST OF TABLES

**Page**

# LIST OF FIGURES

**Page**

# CHAPTER I

# INTRODUCTION

The first chapter contains four parts, including the study's rationale, objectives, hypotheses, and expected outputs. The details of each section are described below.

**Rationale of study**

Inflammatory bowel disease (IBD), a chronic relapsing inflammatory disease of the gastrointestinal tract (GIT) affecting worldwide, most commonly includes Crohn's disease (CD) and ulcerative colitis (UC). The inflammation area of UC is limited to the colon, while CD is most commonly affected in the colon and terminal ileum (2) Although rectal administration offers the shortest route for targeting drugs in the colon, reaching the proximal part of the colon is difficult. Moreover, rectal administration can be uncomfortable and cause patient non-compliance (3). On the other hand, oral administration is often limited by the early drug release before reaching the target site, which may cause drug loss due to acidic and enzymatic degradation in the upper GIT. Consequently, this could result in frequent dosing and side effects from IBD drug therapy, such as peptic ulcers, severe diarrhea, and lymphopenia (4, 5).

As a limitation mentioned above, targeted drug delivery is the way to overcome the limit, which implies selective and effective localization of the drug into the target at therapeutic concentrations with limited access to non-target sites. In the same way, drug therapy aims to supply a therapeutic amount of drug to the target site in a body, which is the desired drug concentration can be therapeutically effective and less toxic (6).

Regarding the local treatment of specific lesions in the colon, the colon drug delivery procedures have focused chiefly on treating colonic diseases because of conventional nontargeted therapies that may result in undesirable side effects. The effectiveness of the drug is essential due to the systemic absorption and distribution

before reaching the target site. Furthermore, the colon drug delivery system is expected to improve the bioavailability of drugs and make them less vulnerable to acidic and enzymatic degradation in the upper gastrointestinal (GI) tract (7). Currently, routes of drug administration to the colon are oral, rectal, or intravenous.

Rectal administration offers the shortest route for specific site of drugs in the colon: however, reaching the proximal part via a rectal route is difficult. Rectal administration can also be uncomfortable for patients, and compliance from patients may not be given effortlessly (8). The parenteral administration also has the same limitations. By way of injection, the parenteral administration route will cause physical discomfort to patients, increasing a patient's non-compliance. Therefore, oral administration is most often considered the more suitable way to administer drugs due to increased patient compliance and reduced physical and mental invasiveness. However, the oral administration is limited by the drug loss due to degradation at the variance pH in the GI tract and a speedy passage through the gastrointestinal tract, leading to low drug bioavailability (4).

The pH-sensitive polymers strategies exploited the variance pH of the GI tract to overcome the previously mentioned limitations (7, 9, 10). The pH-sensitive polymers for colon targeted drug delivery system should be insoluble at low pH levels and increasingly soluble as the pH values in the GI tract change from 1 to 2 in an empty stomach to 5–7 and 6–7.5 in the small intestine and colon, respectively (11-15). For this reason, Eudragit S100 has received attention as a pH-sensitive polymer ideal for a colon-targeted oral drug delivery system (16, 17). Eudragit S100, an anionic copolymer derived from methacrylic acid and methyl methacrylate, is designed to dissolve in neutral or alkaline fluids. This polymer dissolves at pH 7.0 through ionizing its carboxylic functional groups. It thus has been used for targeting drugs in the colonic region of the GI tract, consequential the release of drugs in the colon (18-20).

This pH-sensitive polymer can prevent drug degradation and burst release before reaching the colon. Additionally, it seems sufficient to deliver drugs to the colon via oral administration(21).

Nanostructured lipid carriers (NLCs) are the essential components that can provide the superior performance of drug delivery systems to the colon. NLCs possess unique characteristics formulated by using a combination of solid and liquid lipids that form the amorphous structure of particles in the nanoscale. The NLCs have been proved to be a beneficial system that can be an effective method for colon-targeted oral drug delivery because this formulation can enhance the drug solubility and mucoadhesive property owing to the nanoscale size(22, 23). Therefore, the NLCs can also adhere to the target size, which allows for a prolonged residence time, and sustained release leads to reduced drug administration frequency.

The dual-functional colon-targeted drug delivery system was developed using the drug-loaded NLCs entrapped in pH-sensitive polymers (EudragitS100) beads. In this experiment, curcumin was selected for the drug modeling. Curcumin is a natural compound that has been used for centuries as a dietary supplement and substance used for medical treatment. Curcumin has regained interest due to its pharmacological actions, which is anti-inflammatory, antioxidant, anti-tumor, and anti-proliferative properties. For the inflammatory bowel disease, Curcumin has been demonstrated to inhibit inflammatory compounds (COX-2) by downregulating the expression of NF-kB required for COX-2 activation(1, 24, 25). However, this compound has very low solubility and degradation rate in alkaline aqueous solutions (pH>7.0) due to hydrolysis and oxidation reaction; therefore, this compound is deemed suitable as an indicator for the delivery system development of the unstable drug in the GI tract(26, 27). The colon-targeted drug delivery system is expected to provide maximum therapeutic activity by preventing degradation or the inactivation of a drug during transport to the target site; and, at the same time, minimize the adverse effects because of inappropriate disposition while also diminishing the toxicity of potent drugs by reducing drug dosing.

In conclusion, this study aimed to develop a colon-targeted drug delivery system that consisted of curcumin-NLCs entrapped EudragitS100 beads as a pH-sensitive carrier. Moreover, the physicochemical properties of this formulation also were investigated.

**Objectives of research**

1. To develop a colon-targeted oral drug delivery system of curcumin-loaded nanostructured lipid carrier beads (Curcumin-NLC beads)

2. To study the physicochemical properties of colon-targeted oral drug delivery system of curcumin-loaded nanostructured lipid carrier beads (Curcumin-NLC beads)

**Expected outputs**

Curcumin-NLC beads were prepared by using the ionotropic gelation method. As a colon-targeted oral drug delivery system, curcumin-NLC beads demonstrated early drug release prevention in stomach conditions. Moreover, curcumin-NLC beads exhibited sustained release since pH changes to the alkaline state representing the ileocolonic region.

**Expected outcomes**

Curcumin-NLC beads developed from this study can be used as a specific drug delivery system to the colon via an oral route that can reduce dosing frequency and systemic side effects. Moreover, this formulation can increase patient compliance due to conventional usage than the rectal or parenteral route.

# CHAPTER II

# REVIEWS OF RELATED LITERATURE AND RESEARCH

This chapter provides literature reviews related to this study. The review consists of five parts: structure, Ulcerative colitis, Curcumin, Nanostructured lipid carriers, Colon-targeted drug delivery system, and kinetics of drug release. Each issue is described individually below

**Inflammatory bowel disease (IBD)**

Inflammatory bowel disease (IBD) is a chronic inflammatory disease of the intestine, which can cause debilitating symptoms and negatively impact the patient's quality of life. Two conditions of IBD are characterized by a chronic inflammatory region of the gastrointestinal (GI) tract. Ulcerative colitis (UC) is one of the major types of IBD, a mucosal inflammatory condition confined to the rectum and colon. UC usually is characterized by diarrhea, rectal bleeding, abdominal pain, fatigue, and weight loss. In Crohn's disease (CD), any part of the small or large intestine can be involved and continuous or involve multiple segments (28, 29).

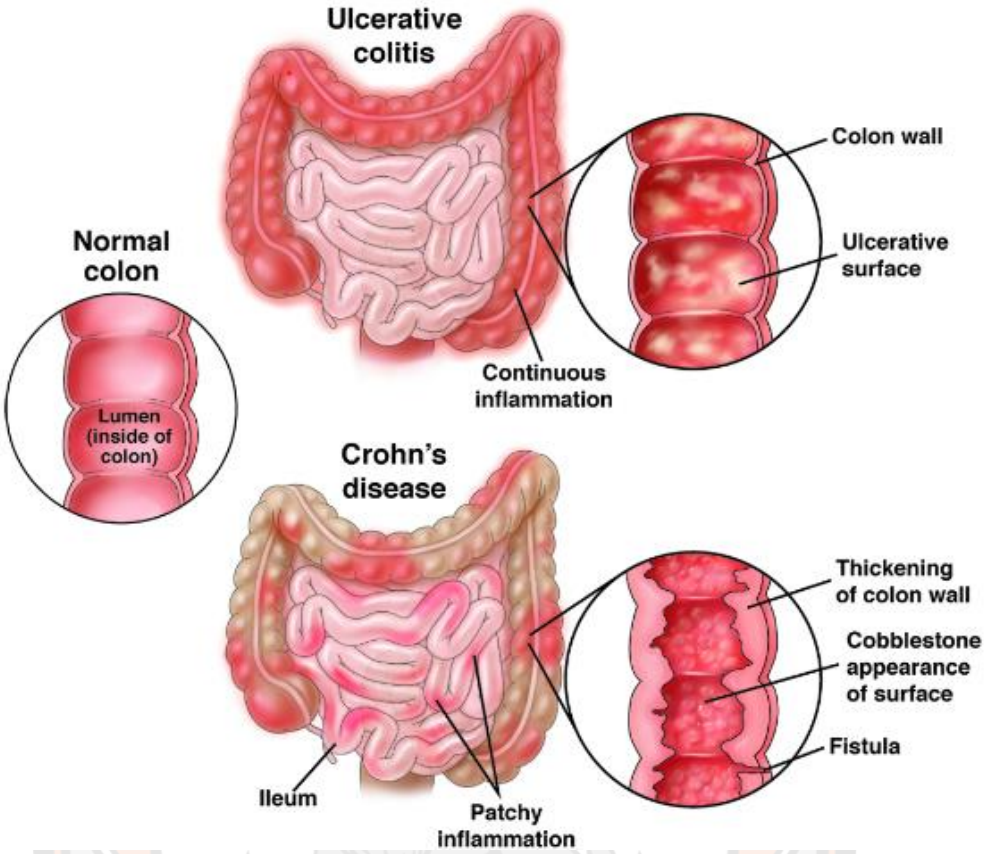


**Figure 1 Characteristics and areas of the colon where ulcerative colitis and Crohn's disease (30)**

**Ulcerative colitis (UC)**

Ulcerative colitis is a lifelong, chronic, disabling inflammatory condition owing to continuous mucosal inflammation of the colon and rectum. UC is not related to an intestinal infection or nonsteroidal anti-inflammatory drug usage. The UC characterization is relapsing and remitting mucosal inflammation, starting in the rectum, and extending to proximal segments of the colon (28, 31).

The incidence of UC is higher in developed countries than in recent decades; in the same way, UC is more frequently diagnosed in urban areas than in rural areas. The incidence of UC in the world varies from 9 to 20 cases per 100,000 people/year, ranging from 11.3 to14.0 per 100,000 people/year in Europe based on data from prospective inception cohorts(31).

The incidence of ulcerative colitis (UC) in Thailand (crude incidence rate of 0.28 per 100,000 persons) is much lower than in the West. Several studies from the high-prevalence area reported that approximately 50% of patients with UC need corticosteroids at ten years(32).

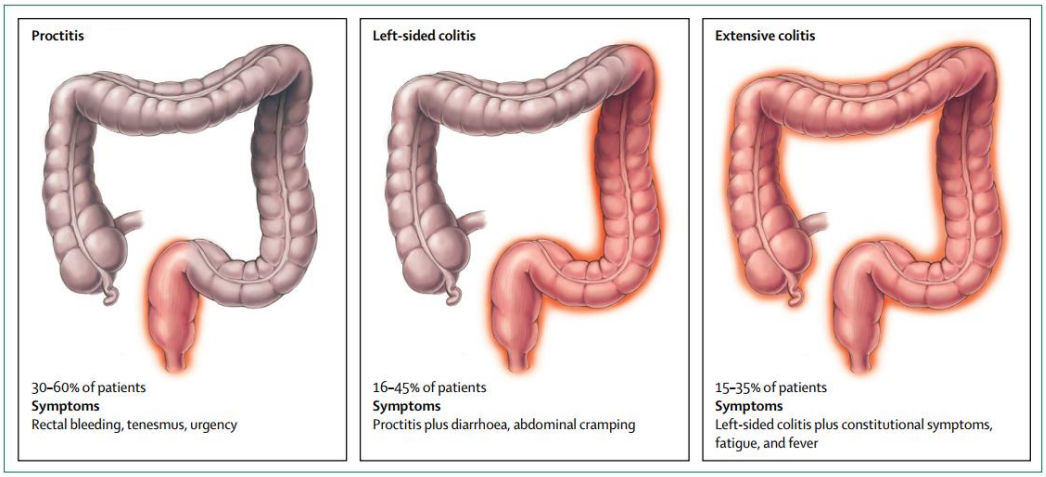


**Figure 2 Ulcerative colitis phenotypes by Montreal Classification ((2)**

**Treatment for UC**

UC's chronic and intermittent inflammation requires long-term combined treatments or an alternative drug. The first purpose of therapy is to reduce symptoms, induce recovery, and maintain this state for as long as possible. Aminosalicylates are the first-line therapy in mild to moderate disease, administered by suppositories, enemas, or oral formulations. Corticosteroids are the most commonly used agents for treating UC patients with moderate to severe activity(33, 34).

**Table 1 Classify and severity of ulcerative colitis by Montreal Classification (35)**

| Montreal classification of extent and severity of ulcerative colitis | | |
|---|---|---|
| **Extent** | | |
| **E1** | Ulcerative procotitis | Involvement is restricted to the rectum (proximal extent of inflammation is distal to the rectosigmoid junction) |
| **E2** | Left-sided UC | Involvement is limited to the portion of the colorectum distal to the splenic flexure |
| **E3** | Extensive UC | Involvement extends proximally to the splenic flexure |
| **Severity** | | |
| **S0** | Clinical remission | Asymptomatic |
| **S1** | Mild UC | Passage of four or fewer stools/day (with or without blood), absence of any systemic illness, and standard inflammatory markers (ESR) |
| **S2** | Moderate UC | Passage of more than four stools per day but with minor signs of systemic toxicity |
| **S3** | Severe UC | Passage of at > 6 bloody stools daily, pulse rate of at least 90 beats/min, the temperature of at least 37.5°C, hemoglobin of less than 10.5 g/100ml, and ESR of at least 30 mm/h |

The patients with remission are treated with aminosalicylates and corticosteroids. Immunomodulating therapy or a biological agent should be considered if it is impractical to taper corticosteroids or frequent relapses occur. Anti-TNF-α drugs are also used in patients admitted to hospital with severe conditions and remained the most widely used biological drugs for UC. Immunomodulators such as azathioprine alone are less effective than infliximab combined to achieve clinical remission(31, 33, 36, 37).

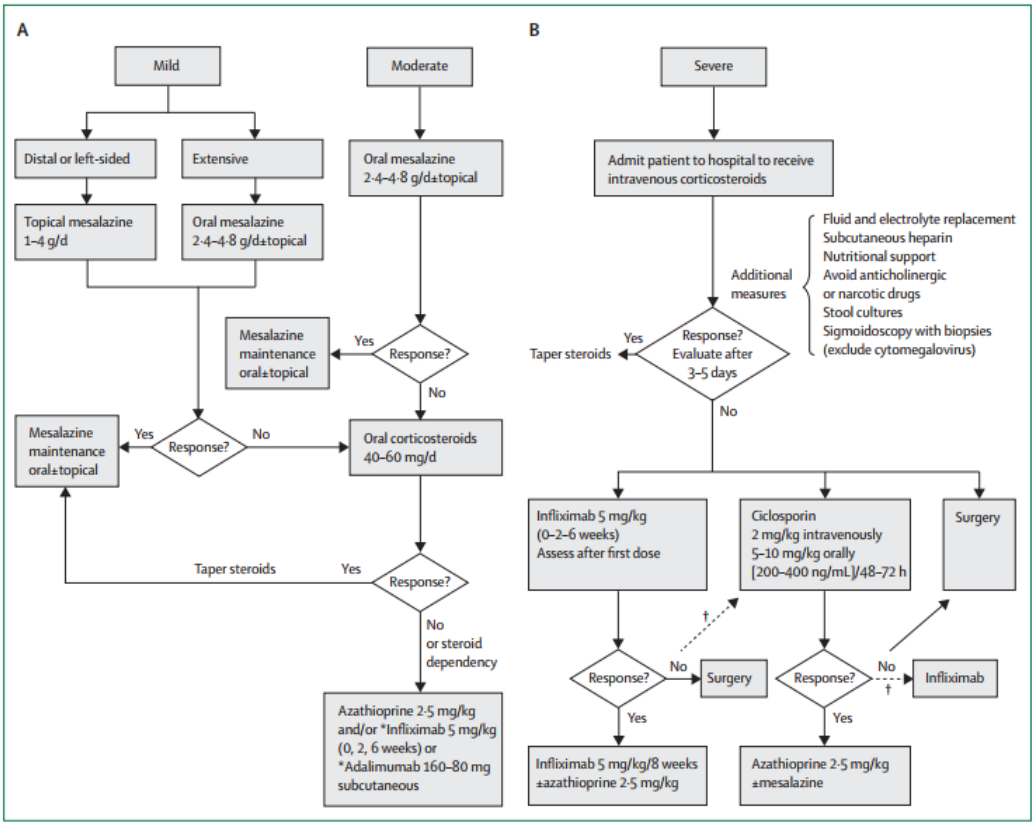


**Figure 3 Treatment algorithm for ulcerative colitis of varying severities (A) mild to moderate ulcerative colitis (B) Severe ulcerative colitis(28)**

**Lack of UC patient medical adherence**

As mentioned before, the treatment requires long-term management to induce and maintain clinical remission; thus, medication adherence is essential for UC patients. Patient adherence can be defined as the extent to which a patient's behavior follows the instructions given by their healthcare physician. However, treatment non-adherence is a common problem among chronic diseases, averaging 50% in developed countries and even poorer in developing countries(38). Non-adherence is one of the significant problems for UC therapy owing to an increase in disease activity, relapse, higher morbidity, and mortality, increased health expenditure, poor quality of life, and higher disability(3). Therefore, this problem is considered a barrier to inducing remission and, therefore, to the patient's clinical improvement(36, 39).

Curiously, the medication regimen is as easy as possible for patients is interesting to determine whether drugs taken on a once-daily basis could deliver results comparable to those obtained with the twice/thrice-daily regimens. The one pilot study followed 22 participants with UC over a 6-month period who were randomized to receive mesalamine either once daily or at the conventional dosing frequency of 2 or 3 times daily. Noticeably, the overall medication consumption was higher with satisfaction in the once-daily dosing group. The findings indicated that reducing drug administration frequency is one proven method of increasing medical adherence to improve clinical outcomes(40).

Additionally, the undesirable adverse effects are frequent reasons for patients' non-adherence. The aminosalicylates reduce inflammation in the lining of the intestine in treating chronic active inflammatory bowel disease and then the maintenance of remission. In most cases, treatment with 5-ASA compounds has been used for UC therapy for several years; side effects occur in up to fifty percent of patients, including nausea, abdominal pain, and headache. These symptoms are remedied by dose reduction. Significantly, sulphasalazine side effects are dose-dependent, especially sulfapyridine produced from sulphasalazine metabolization. Sulfapyridine is absorbed into the systemic circulation(41, 42).

Glucocorticoids are used as the first choice in treating acute flares of UC. In this case, the glucocorticoids effect on inhibition of inflammatory cytokines production and leucocyte function. However, they also have other effects at the therapeutic doses used and various adverse effects, including weight gain, fluid retention, glucose intolerance, hypertension, proximal myopathy, infections, mood changes, cataracts, glaucoma, various skin changes, aseptic bone necrosis, osteoporosis, growth retardation, and adrenal suppression. These side effects are associated with the dose and duration of corticosteroid therapy. If present, most of these side effects will become apparent clinically and reversible on corticosteroid withdrawal(42, 43).

The conventional drug treatment of UC presents several dose-dependent side effects, which can be resolved by drug dosing decreasing or withdrawal. Dose-dependent side effect means the results change when the dose of the drugs is altered; the outcomes are said to be dose-dependent(44).

In addition, route administration is one of the essential factors affecting adherence. The inflammation region of UC involves the rectum and possibly reaches proximally throughout the colon. Therefore, rectal is one of the common routes for UC therapy administration. However, patients appear to prefer oral over rectal administration. The studies described higher adherence to oral 5-ASA than rectal therapy. Consequently, the result suggested that rectal treatment related to non-adherence because of discomfort during use, such as pain or abdominal distension, and inconvenience of administration, such as enemas or suppositories(39, 45).

**Curcumin**

Curcumin is a natural greenish-yellow extract compound from *Curcuma longa*. This compound has been used for many therapies because of its anti-inflammation, antioxidant, etc. Generally, curcumin is an oil-soluble pigment, practically insoluble in water at acidic and neutral pH, soluble in alkaline, and highly susceptible to pH change having a molecular weight of 368.38g/mol and a melting point of 183.0 degrees celsius (46).

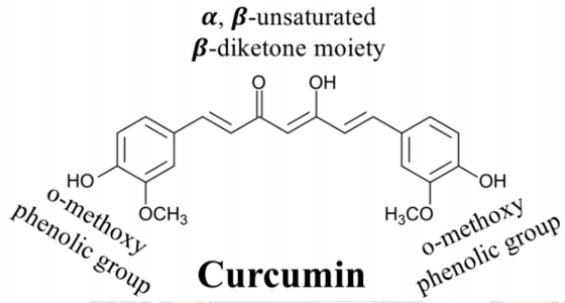


**Figure 4 Curcumin molecule consists of two phenolic groups bonding by diketone moiety (47)**

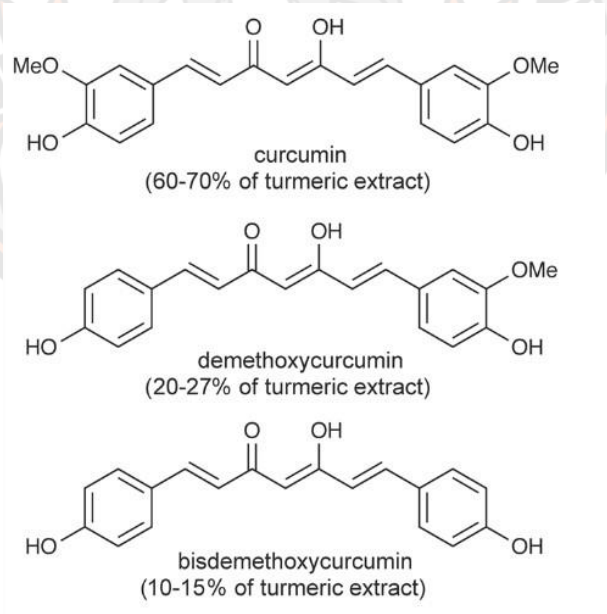


**Figure 5 Major phytoconstituents of extracts of Curcuma longa. This picture demonstrated that curcumin is most compound from Curcuma longa extraction (60-70%) follow by demethoxycurcumin (20-27%) and bisdemethoxycurcumin (10-15%), respectively (48).**

For the chemical degradation of curcumin, the pH of the medium is a significant factor in this situation. In aqueous systems like water, the acidic phenol group donates its hydrogen at alkaline pH, forming the phenolate ion that enables curcumin to dissolve in water. Therefore, curcumin is not stable at neutral and alkaline pH and readily degrades to more minor compounds. Besides, curcumin is derogated due to a chemical autoxidation process (49-51).

**Degradation of curcumin**

**1. Alkaline Degradation**

Curcumin was highly unstable to chemical degradation in alkaline aqueous solutions (pH≥7.0), which has been considered another potential effect of low bioavailability. Under the alkaline condition, the curcumin degradation is notified by the curcumin solution color turning yellow to red via hydrolytic reaction under alkaline conditions. (Fig. 6). In pH range 2-7, most diferuloylmethane species are in neutral form, which is yellow. At pH≥7, the color turns red. The pKa values for dissociating the three acidic protons in compound are determined in Fig 6-7.

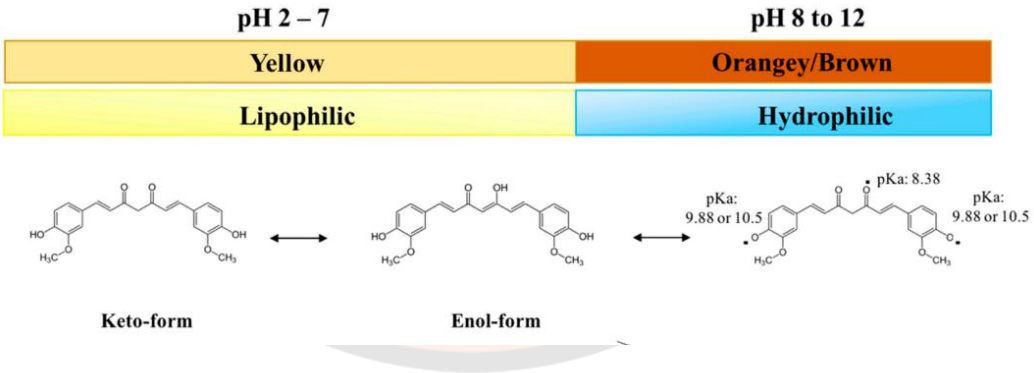


**Figure 6 Curcumin chemically degrades when exposed to alkaline conditions leading to coloring changing and chemical properties (47)**

Wang et al. demonstrated curcumin degradation in phosphate buffer pH 7.4, more than 90% within 30 min. The degraded products are trans-6-(40-hydroxy-30-methoxyphenyl)-2,4-dioxo-5-hexenal, ferulic aldehyde, ferulic acid, feruloyl methane, and vanillin(52). However, the curcumin molecule was relatively resistant to degradation under acidic conditions.

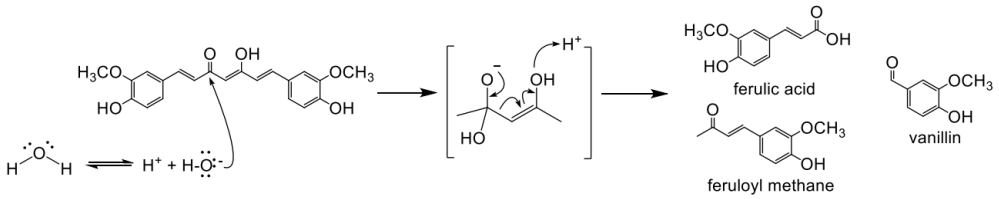


**Figure 7 curcumin can be hydrolyzed into several distinct products, including ferulic acid, feruloyl methane, and vanillin(55).**

The kinetics of curcumin degradation in different pH conditions exhibited first-order kinetics at 37 °C. (Fig.8) Since the observed coefficient ($r^2$) of curcumin degradation in 0.1 N HCl and pH 6.8 or 7.4 phosphate buffer demonstrated the highest correlations in linear regressions for the natural log of the remaining percentage curcumin over time. These results showed that curcumin degradation fitted with first-order kinetic as the $r^2$ were close to 1, indicating that curcumin degradation followed noticeable first-order kinetic. It means that curcumin degradation rates (k) depended on curcumin concentration. Curcumin goes through pH-dependent first-order degradation faster in neutral and alkaline pH (53).

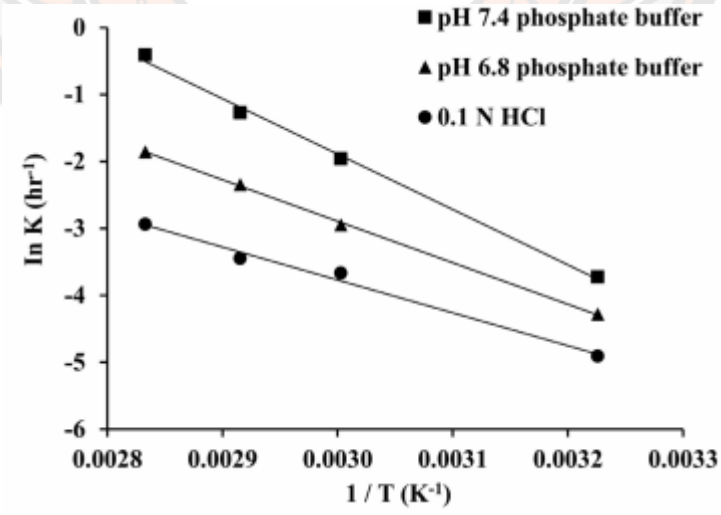


**Figure 8 Arrhenius plot for the first-order rate constant of curcumin degradation in 0.1 N HCl and pH 6.8 or 7.4 phosphate buffer over a temperature range of 37 to 80 °C (53)**

## 2. Photodegradation

Curcumin also undergoes chemical decomposition when exposed to light, which color fades. The photodegradation of curcumin is also begun, which the α, β-unsaturated β-diketone moiety and leads to various reaction products, including p-hydroxybenzaldehyde, vanillin, vanillic acid, ferulic aldehyde, and ferulic acid. Usually, the curcumin powders are more resistant to photodegradation than the solutions, which may be because a higher fraction of the light waves can enter clear solutions(26, 54).

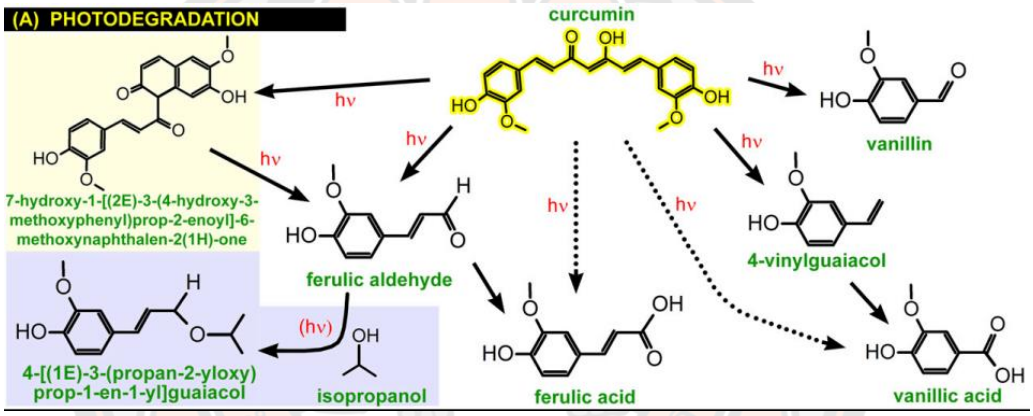


**Figure 9 Photo-induced degradation of curcumin. The demonstrated molecules are byproducts formed during irradiation of solid-state curcumin and curcumin dissolved in an organic solvent, and hν signifies light(26).**

**Pharmacodynamics of curcumin**

Curcumin has recovered interest in recent years due to its pharmacological actions such as anti-inflammatory, antioxidant, anti-tumor, and anti-proliferative properties. The fundamental mechanism by which curcumin intermediates these effects is associated with the activity of suppressing the nuclear factor kappa-light-chain-enhancer of activated B cells (NF-κB). Furthermore, curcumin activity includes suppression of interleukin-1 (IL-1) and tumor necrosis factor-alpha (TNF-α), two major cytokines significant in the regulation of inflammatory responses(55).

Currently, curcumin has also been proposed for digestive diseases such as inflammatory bowel diseases (IBD), a chronic immune disorder affecting the gastrointestinal (GI) tract, which is identified as two major Crohn's disease (CD) and Ulcerative Colitis (UC). The mechanism of action involves inhibition of IKK (IκB kinase), which leads to decreasing cytokine-mediated phosphorylation and degradation of IκB, an inhibitor of NF-κB. After all, the NF-κB inhibition indicates IL-2 synthesis, and IL-2 and mitogen activation of human leukocytes is also inhibited(1, 56).

The clinical trial in UC patients demonstrated significant clinical efficacy of 2 g once daily-dose of curcumin combined with sulfasalazine or mesalamine in the prevention of relapse compared with placebo plus sulfasalazine or mesalamine. The result showed the relapse rate was significantly higher in the placebo group (20.5%) than in the curcumin group (4.7%). There was a statistically significant difference between the percentage of patients with recurrence at six months in the curcumin compared to the placebo group. Moreover, curcumin was well-tolerated and not associated with severe side effects(56). This experiment suggested that adding curcumin had better clinical efficacy than only sulfasalazine or mesalamine in preventing relapse and recurrence of clinical symptoms of UC.

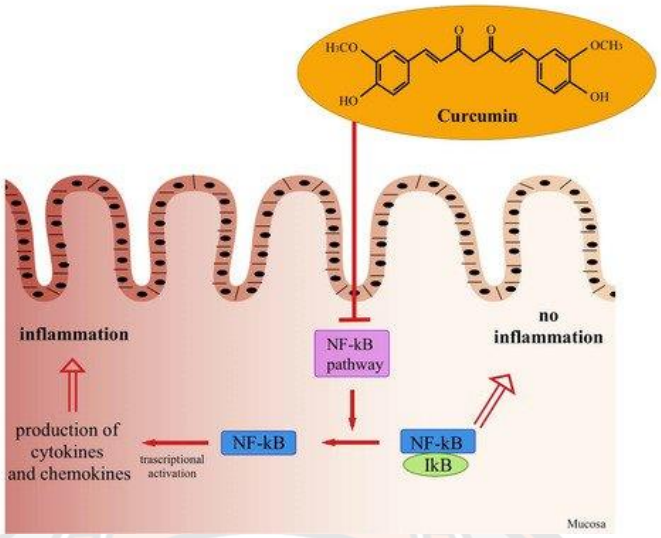


**Figure 10 The anti-inflammatory mechanism of curcumin for idiopathic ulcerative colitis, the pleiotropic effect of curcumin can be the inhibition of activation of the NF-κB signaling cascade level pathway(1).**

**Nanostructured lipid carriers (NLCs)**

Lipid-based nanoparticles containing a solid matrix are generally divided into solid lipid nanoparticles (SLNs) and nanostructured lipid carriers (NLCs). In the early 1990s, SLNs were developed to overcome the limitations of the conventional lipid-based system, in other words, micelles, liposomes, and nanoemulsions; these systems are inclined to degradation during storage and in the GI tract owing to the acidic environment of the stomach, intestinal enzymes, and bile salts. Since SLNs are composed of only solid lipids, the inadequacies are poor drug loading capacity and drug expulsion during storage. NLCs are formulated using a solid and liquid lipid combination resulting in an imperfection matrix to improve these problems. Imperfections between the lipids provide maximum drug-loading capacity due to increased spaces containing the drugs in the matrix. Therefore, NLCs are less susceptible than SLNs during storage (Fig.12) (23, 57-59).

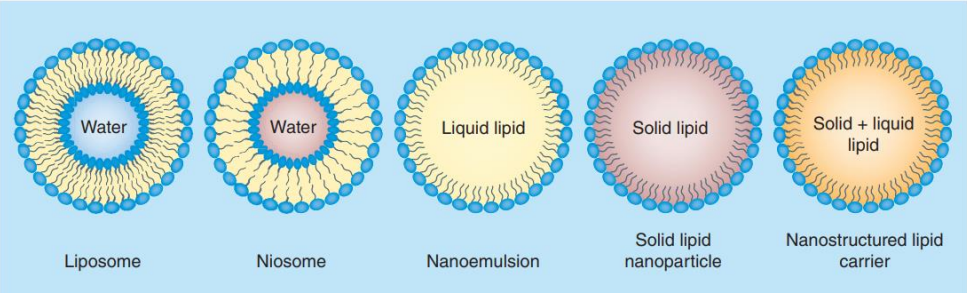


**Figure 11 Various lipid-based systems explored for drug delivery applications**(23)

**Table 2 Comparison between properties of SLNs and NLCs (23)**

| Properties | SLNs | NLCs |
|---|---|---|
| **Drug loading capacity** | Less drug loading capacity due to formation of highly crystalline arrangement | Higher drug loading capacity due to imperfection structure providing higher space |
| **Shelf-life storage** | Drug expulsion takes place during storage due to polymorphic transition | No polymorphic transition takes place, and drug expulsion is prevented |

**Table 3 Advantages of SLNs and NLCs over other nanoparticulate system (59)**

| Parameters | Nano suspensions | Nano emulsions | polymeric nanoparticles | Liposomes | SLNs/NLCs |
|---|---|---|---|---|---|
| Ability to deliver hydrophobic and hydrophilic drug | only hydrophobic drugs | Yes | Yes | Yes | Yes |
| Physical stability | Good | Moderate | Good | Poor | Good |
| Biological stability | Moderate | Moderate | Good | Poor | Moderate |
| Biocompatibility | Moderate | Good | Moderate | Good | Good |
| Drug targeting | Poor | Poor | Moderate | Moderate | Moderate |
| Drug loading | High | High | Moderate | Low to moderate | High |
| Ability to deliver biotechnological | No | Poor | Moderate | Moderate | Moderate |
| Oral delivery | Possible | Possible | Possible | Not Possible | Possible |
| Parenteral delivery | Possible | Possible | Possible | Possible | Possible |

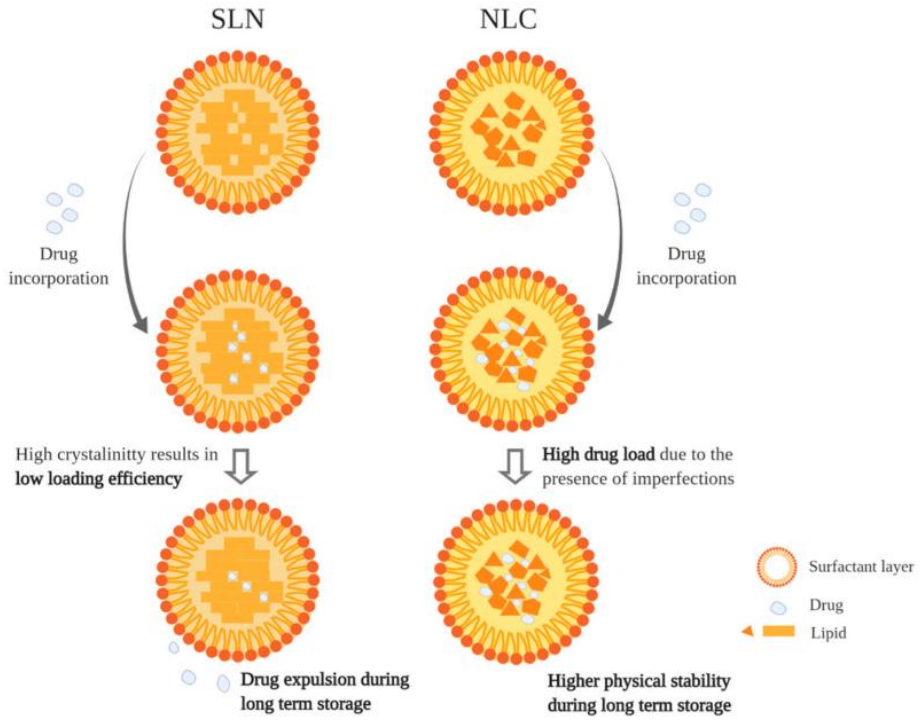


**Figure 12 SLNs and NLCs drug loading different (57)**

As pointed out, NLCs overcome the disadvantages associated with SLNs. In other words, they perform higher drug loading and storage stability. The three types of NLCs structure were considered depending on the production method and the lipid blend composition: imperfect type, amorphous or structureless type, and multiple type (Fig 13) (60, 61). In imperfect type, the matrix of the NLCs cannot form a highly ordered structure resulting in structural defects due to the different chain lengths of the various fatty while preparations. The amorphous type, particularly lipids, cannot recrystallize after homogenization and cooling. Hydroxyoctacosanylhydroxystearate, isopropyl myristate, and dibutyl adipate are generally used to formulate this type. In multiple type, the solid lipids are blended with oils, such as medium and long-chain triacylglycerols, with a ratio that surpasses the solubility of the oil molecules in the solid lipid. The tiny oil droplets formation is exhibited due to the lipid droplets reaching the miscibility gap, resulting in oil precipitation in the cooling process (62).

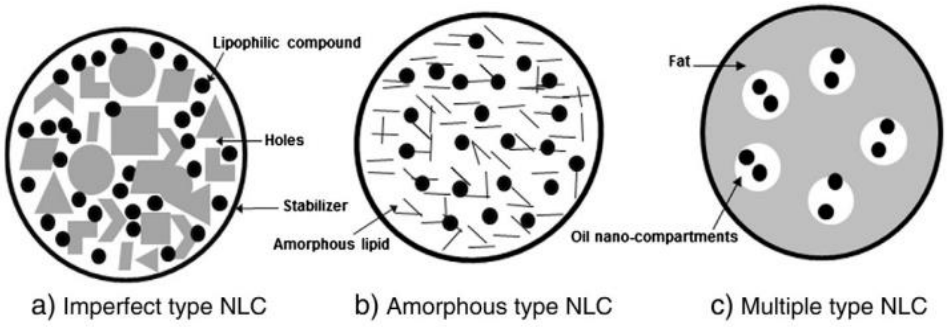


**Figure 13 Types of NLCs depend on the lipid matrix structure (61)**

**The advantages of NLCs**

**Poorly soluble drugs**

Appropriate drug solubility at the absorption site is necessary for achieving acceptable oral bioavailability. However, more than 40% of new chemical entities from combinatorial screening programs are poorly aqueous soluble, which is a significant concern to formulation scientists. NLCs have an inherent GI solubilization capacity due to the change of the crystalline form of the drug into amorphous form, high dissolution velocity due to their small size, and utilization of a selective lymphatic transport system. Thus, NLCs have been widely implicated in this arena to facilitate the solubilization of various lipophilic agents.

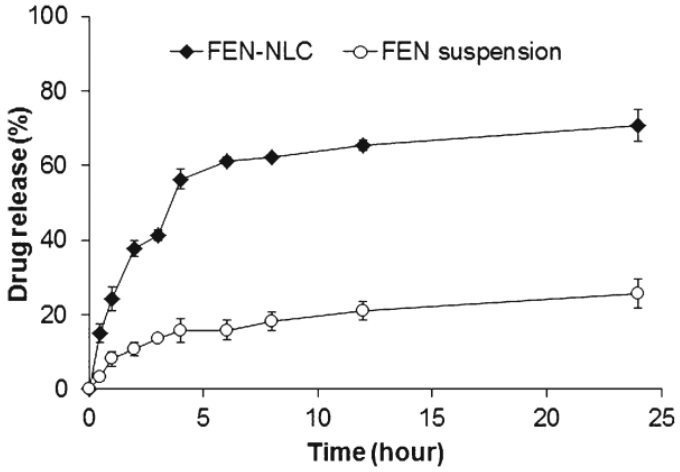


**Figure 14 In vitro drug release of fenofibrate from fenofibrate loaded NLCs and fenofibrate suspensions in water (63).**

Tuan Hiep Tran et al. showed that fenofibrate-NLCs could improve low water solubility compared with suspensions. Approximately 60% of the drug was released from formulations in the first four h, followed by gradual release up to 24 h(Fig.14). Similarly, compared with its suspension, an improved dissolution profile was examined for fenofibrate-loaded NLCs. The result exhibited a four-fold improvement in the area under curve (AUC) values in orally administered rats (63).

**Stabilization of drugs**

The orally consumed substance is exposed to fluctuating conditions in different sections of the GI tract, which can adversely affect the stability of medicine. For example, the stomach pH instability drug will be degraded before the target reaches.

Na Zhang et al. reported the remaining percentage of insulin after incubating insulin-loaded SLNs in pepsin solution. The remaining insulin after incubation in trypsin solution of insulin-loaded SLNs was significantly greater than solutions. Insulin-loaded SLNs revealed better stability than insulin solution under investigational conditions. Therefore, SLNs are considered stable oral administration carriers due to their outstanding protection against acidic pH and enzymatic degradation (64).

**Colon-targeted drug delivery system**

Targeted delivery of remedial to the colon is useful for Colon diseases, including ulcerative colitis, Crohn's disease, irritable bowel syndrome, and colon cancer (65). This targeted system is exploited for the drugs that are degraded by the stomach's acidic environment or metabolized by pancreatic enzymes and are only slightly affected in the colon. Therefore, colon-targeted oral drug delivery is an active area of research for local diseases disturbing the colon. It increases the efficacy of therapeutics and allows localized treatment, which minimizes systemic adverse effects. The oral-colon drug targeted administration is achieved in various ways: pH-sensitive, time-controlled release systems, and microbially triggered drug delivery (66). Colon-targeted drug delivery facilitates direct treatment in the disease region, reduces dosing frequency, and decreases the risk of systemic adverse effects.

The oral administration is the greater convenient and preferred; however other pathways for colon-targeted drug delivery may also be used. The rectal route offers the

shortest way to target drugs in the colon. Nevertheless, getting the proximal part of the colon via rectal administration is also complicated. Rectal administration can also be uncomfortable, which affects medical adherence leading to undesirable therapeutic effectiveness (39, 45). Drug formulation for intrarectal administration is enemas, foam, and suppositories. The rectal route is used both for systemic dosing and drug delivery to the colon.

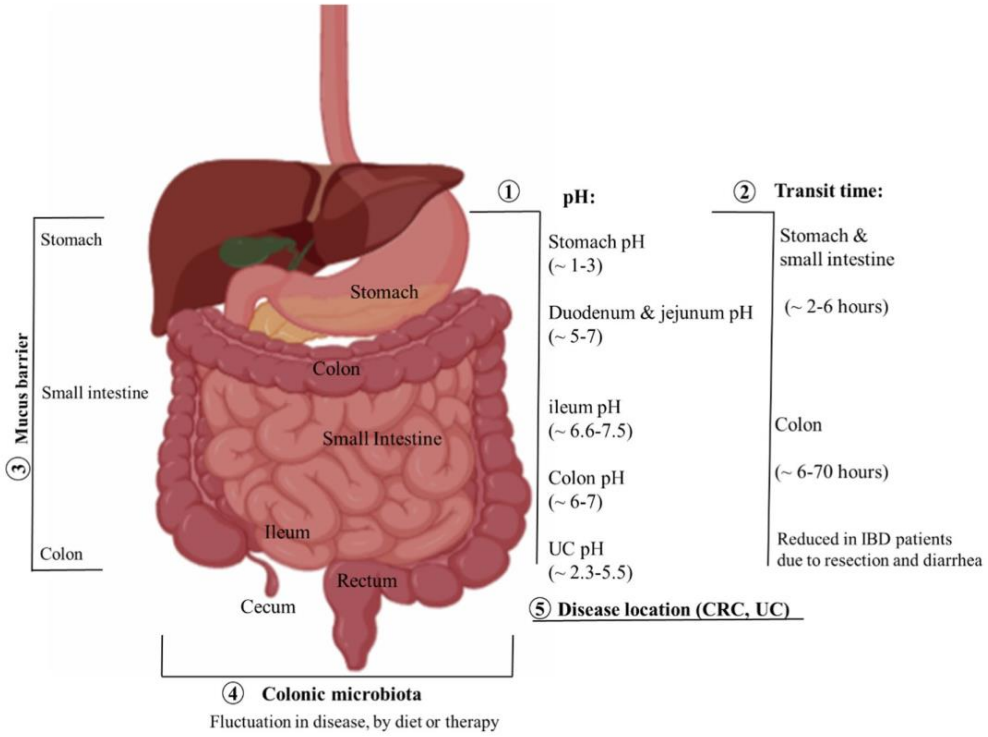


**Figure 15 Considerations related to colonic drug delivery. Physiological and pathological factors such as pH variations, changes in GI transit time, mucus barriers, disease location in the colon, and microflora variability between healthy and diseased individuals can affect colon-specific drug delivery (67)**

**Table 4 Criteria for selection of drugs for colon-targeted drug delivery system (68)**

| Criteria | Pharmacological class |
|---|---|
| Drugs used for local influences in the colon against GIT disease | Anti-inflammatory drugs |
| Drugs poorly absorbed from upper GIT | Anti-hypertensive and Antianginal drugs |
| Drugs that degraded in the stomach and small intestine | Peptides and proteins structure of drugs |
| Drugs that undergo extensive first-pass metabolism | Nitroglycerin and corticosteroids |

**Approaches for achieving a colon-targeted drug delivery system (CDDS)**

Numerous techniques are used for site-specific drug delivery. Among the primary strategies for Colon-targeted drug delivery include:

**Time-dependent release system**

A time-dependent release system has also been anticipated as an approach targeting the large intestine. For the colonic release accomplishment, the lag time should balance the time the system takes to obtain the colon. The time is difficult to predict in advance, even though a lag time is described as relatively persistent at three to four hours (65, 69).

**Table 5 The transit time of the gastrointestinal tract (70)**

| Organ | Transit time (hour) |
|---|---|
| **Stomach** | Fasted state < 1<br>Fed state >3 |
| **Small intestine** | 3 - 4 |
| **Large intestine** | 20 – 30 |

This approach is uninfluenced by the individual variance in the pH of the digestive system or the intestinal bacteria. These systems carry the drugs by divergent mechanisms such as osmosis, swelling, or a combination of both. Enteric-coated time-release tablets are comprised of three layers, a drug in the tablet core (immediate release part), the coated swellable hydrophobic polymer layer (time release part), and an enteric coating layer (acid resistance part). The release of tablets does not occur in the stomach due to the acid resistance of the outer enteric coating layer. After passing the stomach, the enteric coating layer performs dissolves.

Moreover, the intestinal fluid begins to erode the coated polymer layer slowly. There is no drug release after passing the stomach. However, at the ileocolonic area, after erosion reaches the core tablet and exhibits rapid release. The lag time duration depends on either the weight or composition of the polymer layer (68, 71, 72).

**Microbially Triggered Drug Delivery to Colon**

These techniques depend on exploiting the specific enzymatic activity of the enterobacteria current in the colon. The colonic bacteria are mainly anaerobic in the environment and secrete enzymes that are efficient in metabolizing compounds such as carbohydrates and proteins that leak the digestion in the upper GI tract. The enzymes that appear in the colon are reducing enzymes (Nitroreductase, Azoreductase, N-oxide reductase, sulfoxide reductase, Hydrogenase) and hydrolytic enzymes (Esterases, Amidases, Glycosidases, Glucuronidase, sulfatase). The susceptibility to degradation by bacterial enzymes within the colon can be applied as a vehicle for drug delivery to the colon. This anchor has been exploited to deliver 5-aminosalicylic acid to the colon as a prodrug carrier. The prodrug sulphasalazine comprises two separate molecules, sulphapyridine, and 5-aminosalicylic acid, coupling by an azo bond. The host bacteria enzymes split the azo bond and disentangle the sulphapyridine and therapeutic agent 5-aminosalicylic acid. This idea accompanies the development of an azo-bond polymer for obtaining specific carrier systems. Despite that, the safety and toxicity of these synthetic polymers are still concerns. To overcome this problem, natural materials, which are polysaccharide-based, are a suitable alternative to the situation. Materials comprise chondroitin sulfate, chitosan, guar gum, amylase, dextran, and pectin. These

materials are hydrophilic, making them soluble or conduct to swelling in an aqueous environment, according to inappropriate drug carriers(66, 69, 73, 74).

**pH-dependent system**

As it is well known, the luminal pH varies from highly acidic in the stomach to a slight basis in the intestine. Such pH variations can cause pH-induced oxidation, deamidation, or hydrolysis of peptide and protein drugs, leading to the loss of their activity. The pH-sensitive polymers have been attention-delivered drugs to the small intestine and colon to overcome the undesirable pH. These polymers are insensitive to acidic conditions of the stomach and dissolve in the higher pH environment of the small intestine. The pH differential principle of the GI tract has also been attempted for ileocolonic delivery purposes. The most commonly co-polymers of methyl acrylic acid and methyl methacrylate that dissolve at a slower rate and a higher threshold pH (pH 7 -7.5) have been developed recently.

The stomach's pH ranges between 1 and 2 and increases during the fed state. The pH is 6.5 in the proximal small intestine and 7.5 in the distal small intestine, more and less. The pH in the colon is 6.6 and 7.0 in the descending colon (75). The use of pH-sensitive polymers depends on these differences in pH levels. The polymers designated as pH-sensitive in colon-specific drug delivery are insoluble at a low-level pH stage and increasingly soluble as pH rises. Although a pH-sensitive polymer can defend a formulation in the stomach and proximal small intestine, it may begin to dissolve in the lower small intestine and then release the drug in the ileocolic region. Therefore, the formulations can be ileocolonic site-specificity by using pH-sensitive polymers (7, 66, 68, 74).

**Eudragit®**

Poly(meth)acrylates are known globally by the marketing name Eudragit®. The flexibility to merge the different polymers makes it possible to accomplish the desired drug release profile by releasing the drug at the proper place, at the precise time, and, if necessary, over the selected period. Other essential functions are protected from external influences(76).

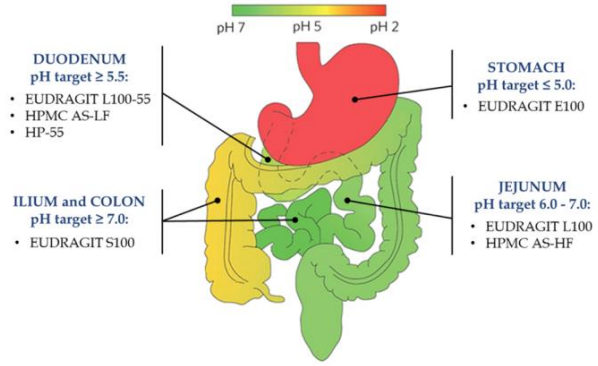


**Figure 16 Schematic showing different polymers used to target drugs in the human gastrointestinal tract (77).**

The most employed Eudragit grades include Eudragit L 100 and S 100. Eudragit L dissolved at pH > 6 and is used for enteric coating. In contrast, Eudragit S, which dissolves at pH >7 (attributed to the presence of the higher amount of esterified groups in relation to carboxylic groups), is used for colon targeting. The ratio of methacrylic acid to methyl methacrylate is 1:2 in Eudragit S (78).

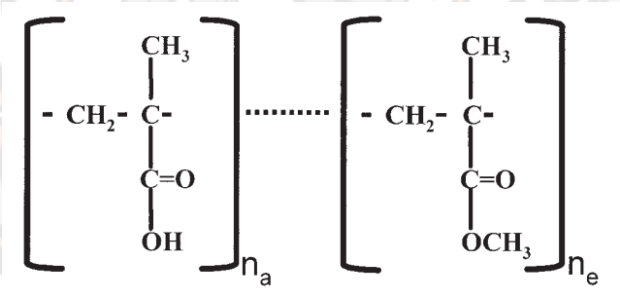


**Figure 17 Main structure of Eudragit type L and S polymer, which two major functional groups, carboxylic group and ester group(79)**

These can either target the release of the drug in the proximal small intestine (enteric coating) or the colon. The enteric coating can be attained by coating the dosage form with an ionizable carboxylic acid group-containing weakly acidic polymer that will break down only at the basic pH of the small intestine while remaining intact in the stomach. Eudragit can dissolve in the range of 6.8 to 7.5 and may be used for colonic delivery (79). Thus, the site-specific delivery of drugs to different regions.

**Kinetic drug release**

The administration of a drug has the main objective of enabling the action for which it is intended. The conventional therapeutic regimens often use a high amount of a drug, with a high fraction excreted without exerting activity. According to the definition, modified drug release means that the active agent's release differs from traditional release. Therefore, drug release is an essential property of a drug delivery system, constituting an effect on the absorption of the therapeutic agent. Thus, controlled release dosage forms enable pharmacists to design controlled drug delivery systems(80, 81).

Consequently, it is necessary to know the exact mass transport mechanisms involved in drug release and to predict the resulting drug release kinetics quantitatively. It is possible to employ a mathematical equation that describes the dependence of release on the function of time, leading to many models used to design several simple and complex drug delivery systems and devices and to predict the overall release behavior. It is essential to know how to use these equations to understand the several factors that affect dissolution velocity and how dissolution behaviors can vary and influence the efficiency of the therapeutic regimen of patients. Mathematical equations enable the quantitative interpretation of the values obtained from a dissolution or drug release assay(82).

However, based on different mathematical functions, model-dependent methods are beneficial in describing the release profile. Once a suitable function has been selected, the dissolution profiles are evaluated depending on the derived model parameters. The main-release kinetic models are zero order, first order, Higuchi, Korsmeyer–Peppas, and Hopfenberg.

**Zero-order model**

For zero-order kinetics, the release of an active agent is only a function of time, and the process takes place at a constant rate independent of active agent concentration. Thus, zero-order kinetics defines the process of constant drug release from the drug delivery system, and drug level in the blood remains constant throughout the delivery. This relationship can describe the drug dissolution of several types of modified release pharmaceutical dosage forms, as in the case of some transdermal systems, matrix tablets with low soluble drugs in coated forms, osmotic systems, etc. The pharmaceutical dosage forms following this profile release the same amount of drug by a unit of time and are the ideal drug release method to achieve a prolonged pharmacological action. The following relation can, in a simple way, express this model:

$$\mathbf{M_t = M_0 + k_0 t} \qquad \textbf{... (Equation 1)}$$

Where $M_t$ is the amount of drug dissolved in time t, $M_0$ is the initial amount of drug in the solution (most times, $M_0 = 0$), and $k_0$ is the zero-order release constant. Hence, the drug release kinetics data obtained from the *in-vitro* dissolution study is plotted against time, i.e., cumulative drug release *vs.* time(83).

**First-order model**

This model has been used to describe the absorption and/or elimination of various therapeutic agents. In this sense, first-order release kinetics states that change in concentration to change in time depends only on concentration. The equation can represent the release of drug which follows first-order kinetics:

$$\log M_1 = \log M_0 + \frac{k_1 t}{2.303} \qquad \text{... (Equation 2)}$$

Where $M_1$ is the amount of drug released in time t, $M_0$ is the initial amount of drug in the solution, and $k_1$ is the first order release constant. In this way, a graphic of the decimal logarithm of the released amount of drug versus time will be linear. The pharmaceutical dosage forms following this dissolution profile, such as those containing water-soluble drugs in porous matrices, release the drug in a way that is proportional to the amount of drug remaining in its interior so that the amount of drug released by a unit of time diminishes(84).

**Higuchi model**

This model was developed to study the release of water-soluble and low-soluble drugs incorporated in semi-solid and/or solid matrixes, which means releasing a drug from the drug delivery system involves dissolution and diffusion. Mathematical expressions were obtained for drug particles dispersed in a uniform matrix behaving as the diffusion media. Generally, it is possible to resume the Higuchi model to the following expression:

$$M_t = k_H \times t^{1/2} \qquad \text{... (Equation 3)}$$

Where $M_t$ is the cumulative amount of drug released in time t per unit area, $K_H$ is the Higuchi dissolution constant. The data obtained were plotted as cumulative percentage drug release versus square root of time. Therefore, the simple Higuchi model will result in a linear M versus $t^{1/2}$ plot having a gradient, or slope, equal to $K_H$, and we say the matrix follows $t^{1/2}$ kinetics(85).

**Korsmeyer-Peppas model**

The power law model helps study drug release from polymeric systems when the release mechanism is unknown or when more than one type of phenomenon of drug release is involved. It can be seen as a generalization of the observation of the superposition of two independent mechanisms of drug transport, relaxation and diffusion. The release data were fitted using the well-known empirical equation proposed by Korsmeyer and Peppas.

$$\frac{M_t}{M_{inf}} = kt^n \quad \text{... (Equation 4)}$$

Where $M_t$ is the amount of drug released in time t, $M_{inf}$ is the amount of drug released after time infinite, $M_t/M_{inf}$ is a fraction of drug released at time t, k is the release rate constant, and n is the release exponent in the function of time t. The n value is used to characterize different releases (Table 7)(86, 87).

**Table 6 Interpretation of diffusional release models of active agent from polymeric matrices with different geometries**

| Drug transport mechanism | Geometry | Release exponent (n) | Time in a function of n |
|---|---|---|---|
| **Fickian diffusion** | Planar | 0.5 | $t^{0.5}$ |
| | Cylinders | 0.45 | $t^{0.45}$ |
| | Spheres | 0.43 | $t^{0.43}$ |
| **Anomalous transport** | Planar | 0.5<n<1.0 | $t^{0.5<n<1.0}$ |
| | Cylinders | 0.45<n<0.89 | $t^{0.45<n<0.89}$ |
| | Spheres | 0.43<n<0.85 | $t^{0.43<n<0.85}$ |
| **Case-II transport** | Planar | 1.0 | $t^{1.0}$ |
| | Cylinders | 0.89 | $t^{0.89}$ |
| | Spheres | 0.85 | $t^{0.85}$ |
| **Super Case-II transport** | Planar | n>1.0 | $t^{n>1.0}$ |
| | Cylinders | n>0.89 | $t^{n>0.89}$ |
| | Spheres | n>0.85 | $t^{n>0.85}$ |

**Hopfenberg model**

Hopfenberg developed a mathematical model to correlate the drug release from surface eroding polymers so long as the surface area remains constant during the degradation process. The cumulative fraction of drug released at time t was described as:

$$\frac{M_t}{M_{inf}} = 1 - \left[1 - \frac{k_0 t}{C_0 a_0}\right]^n \quad \text{... (Equation 5)}$$

Where Mt is the amount of the drug released at the time t, $M_{inf}$ is the amount released at the infinite time, $M_t/M_{inf}$ is a fraction of the drug dissolved. $k_0$ is the erosion grade constant, $C_0$ is the initial concentration of the drug in the matrix, and $a_0$ is the initial radius of the sphere or cylinder or a half part of the thickness of the flim. According to the geometrical form, the n value is 1, 2, or 3 for the flim, cylinder, or sphere. This model separately shows the characteristics of diffusion and relaxation of permeability. The limiting factors for drug release are matrix erosion and time, which depend on internal and external diffusing resistance(88).

# CHAPTER III

# RESEARCH METHODOLOGY

This chapter presents the experimental design, including materials, apparatus, and methods. Each topic is described individually below.

## Materials

1. 95% ethanol (Analytical grade, RCI Labscan, Bangkok, Thailand)
2. Acetonitrile (HPLC grade, Lab-scan Ltd,
3. Calcium chloride ($CaCl_2$) (Ajax Finechem, New South Wales, Australia)
4. Curcumin extract (lot no.19031229-1, Thai-China Flavours and Fragances Industry Co., Ltd, Bangkok, Thailand)
5. Curcumin standard (lot no. SLBB7593V, Sigma, Bangkok, Thailand)
6. Eudragit® S100 (Evonik, Darmstadt, Germany)
7. Eudragit® L100 (Evonik, Darmstadt, Germany)
8. Fasted-State Simulated Gastric Fluid (FaSSGF) (Biorelevant.com Ltd, UK)
9. Fasted State Simulated Intestinal Fluid (FaSSIF) (Biorelevant.com Ltd, UK)
10. Glacial acetic acid (Analytical grade, RCI Labscan, Bangkok, Thailand)
11. Glyceryl monostearate (Namsiang trading Co., Ltd, Bangkok, Thailand)
12. Hydrochloric acid 37% (AR grade, RCI Labscan, Bangkok, Thailand)
13. Mannitol (Ajax Finechem, New South Wales, Australia)
14. Medium-chain triglyceride (Lexol® GT865, Namsiang trading Co., Ltd, Bangkok, Thailand)
15. Membrane filter (Cellulose acetate, pore size 0.22 µm, diameter 25 mm, Millipore Corporation, Massachusetts, USA)
16. Nitrogen gas
17. Polyoxyethylene (20) sorbitan monooleate (Tween 80, Ajax Finechem, Australia)
18. Potassium chloride (RCI Labscan, Bangkok, Thailand)

19. Potassium dihydrogen orthophosphate (RCI Labscan, Bangkok, Thailand)
20. Sodium bicarbonate (RCI Labscan, Bangkok, Thailand)
21. Sodium sulfosuccinate (AOT) (Fluka, USA)
22. Sodium chloride (RCI Labscan, Bangkok, Thailand)
23. Soybean phospholipids (Emulmetik® 900, Lucas Meyer, Champlan, France)
24. Stearic acid (Namsiang trading Co., Ltd, Bangkok, Thailand)
25. Ultrafiltration YM100 membrane (Regenerated cellulose, Cut off 100 kDa, Diameter 76 mm, Millipore, USA)

**Equipment**

1. Analytical balance (TB-214, Denver instrument, Germany)
2. Column HPLC (150 x 4.6 nm reversed phase C18 column, Gemini, Phenomenex®, Torrance, USA)
3. High-speed Centrifuge (MIKRO 120, HET-1 1204, Hettich, Germany)
4. High-speed homogenizer (Model AX5, SILVERSON, England)
5. Homogenizer (Ultra-Turrax T25, KIKA-Laboratechnik, Germany)
6. High-pressure liquid chromatography (HPLC, Model LC-20AT, Shimadzu, Kyoto, Japan)
7. Lyophilizer (Lyolab 3000, Heto, Thermo Fisher Scientific Inc., MA, USA)
8. Magnetic stirrer (Model C-MAG HS7, IKA-1 3581200, IKA, China)
9. Particle size analyzer (Zeta PALS, ZetaPAL® Brookhaven instruments corporation, New York, USA)
10. Peristalsis pump (BECKTHAI BANGKOK EQUIPMENT & CHEMICAL Co., Ltd., Bangkok, Thailand)
11. pH meter (Model delta 320, Mettler-Toledo, Shanghai, China)
12. Transmission electron microscopy (Model Tecnai 12, Philips, Oregon, USA)
13. Ultrafiltration cell (Model 8400, Amicon Grace company, Beverly, MA, USA
14. Ultrasonic Probe (VCX130-Sonic, Sonic & Material inc, Newtown, CT, USA)
15. UV-Vis Spectrophotometer (Model GENESYS 10S UV-VIS, Thermo Scientific, USA)
16. Vortex mixer (Model Vortex-2 genie, Becthai CO., LTD, Bangkok, Thailand)
17. Water bath (MS 20, Lauda, Germany)
18. Zeta potential analyzer (Zetaplus, Brookhaven, New York, USA)

**Methodology**

**Preliminary study**

**The Eudragit S100 solubility in 0.2 M NaOH and bead formation study**

The solubility of various Eudragit S100 concentrations was determined by dissolving ES100 powder in a concentration of 1%, 3%, 5%, and 10% in 0.2 NaOH solution. Then, homogeneously mixed by a magnetic stirrer at 500 rpm. After that, the solubility of ES100 in each concentration was observed. After that, for bead formation determination, the Eudragit solution in each concentration was dropped into the 1.0 N HCl solution. Then the bead formation was observed.

**The ES100 beads formation study by ionotropic gelation method**

To find the suitable concentration and ratio of Eudragit (e.g., Eudragit S100; ES100 and Eudragit L100-55; EL100) for the bead formation, the Eudragit solutions with variance concentration were dropped in 50 mL of 5%, 10% (w/v) $CaCl_2$ dissolved in 1 M HCl under continuous stirring at 500 rpm at room temperature. The beads were washed three times with deionized water and dried on a watch glass at 60 degrees celsius.

**The ES100 beads dissolution study**

The Eudragit beads were performed in Phosphate buffer pH 6.8 and Phosphate buffer pH 7.4. The beads were dispersed in a dissolution medium at 37.0 ± 0.5 ºC and shaken at level 1 of the water bath (MS 20, LADUA, Germany). Then, the Eudragit beads dissolution was observed.

**High-performance liquid chromatography (HPLC) analysis for curcumin**

Curcumin was analyzed by the HPLC method. The HPLC system consisted of an LC20-AT pump connected to a SIL-10ADVP auto-injector, an SPD-6AV system controller, and SPD-20A UV-visible detector. Curcumin was separated using a Vertisep C18 column (5 µm, 4.6 x 250 mm) and a guard column. The mobile phase was prepared by mixing acetate buffer and acetonitrile at a ratio of 50:50 (v/v). A flow rate of 1.2 ml/min and a detection wavelength of 425 nm was employed. The dissolved curcumin was quantified with a calibration curve of standard curcumin in a concentration range of 0.1-10.0 µg/ml.

**Curcumin-loaded nanostructured lipid carrier (curcumin-NLCs) preparation**

Curcumin-NLCs were prepared by a warm microemulsion technique, as previously reported by Chanburee S. and Tiyaboonchai W. (89). Briefly, the water phase consisted of curcumin, AOT, Tween 80, and deionized water, heated to ~75°C before adding into the oil phase. The oil phase, consisting of phospholipids, glyceryl monostearate, medium-chain triglyceride, and stearic acid, was heated to ~75°C. The warm microemulsion was dispersed in cold water under a high-speed homogenizer (Model AX5, Silverson, England). The Curcumin-NLCs dispersion was washed three times with deionized (DI) water using an ultrafiltration cell fitted with an MWCO 100 kDa membrane. Finally, 4% (w/v) mannitol was added to the curcumin-NLCs dispersion before being frozen and lyophilized for 72 h at $1\times10^{-4}$ Torr and - 55°C by Freeze-dryer (GAMMA 2-16 LSCplus, Christ, Germany).

**Curcumin-NLC beads preparation**

The curcumin-NLC beads were prepared by using the ionotropic gelation technique. Briefly, the ES100 solution was prepared by dissolving ES100 in 0.2 N NaOH. The curcumin-NLCs were dispersed in 20 mL of ES100 solution before dropping into 50 mL of 10% (w/v) $CaCl_2$ dissolved in 1 M HCl under continuous stirring at 500 rpm at room temperature. The obtained beads were washed three times with DI water and dried in a hot air oven at 40°C for two days. Two formulations were prepared by varying the amount of ES100 in the 7ES to 7% (w/v) and 9% (w/v) for the 9ES.

**Physicochemical characterization of curcumin-NLCs**

**Mean size and size distribution**

The mean particle size and polydispersity index (PI) were measured by dynamic light scattering with a ZetaPALS® analyzer (Zetaplus, Brookhaven, New York, USA) equipped with a 35 mW, 632.8 nm. HeNe laser diode and a BI-200SM goniometer connected to a BI-9010AT digital correlator. Samples were diluted with DI water before measurement. The measurements were performed in triplicate.

**Surface charge determination**

The surface charge was determined by phase analysis light scattering employing a ZetaPALS® analyzer. Samples were diluted with DI water before measurement in triplicate. After that, zeta potential was calculated for electrophoretic mobility using the Smoluchowski equation.

**Physicochemical characterization of curcumin-NLC beads**

**Mean size of curcumin-NLC beads**

The mean size of the curcumin-NLC beads was carried out using a sieving analyzer (AS200, RETSCH, Bangkok, Thailand). At least 3 grams of sample were sieved through several progressively finer mesh sieves (mesh No. 15-25) via mechanically shaking for 5 minutes. Afterward, the percentage of the retained mass of each sieve was determined followed by this equation:

$$\textbf{Mean diameter(mm.)} = \frac{\sum nd}{\sum n} \qquad \textbf{... (Equation 6)}$$

n; the weight of the bead in each sieve

d; diameter size of sieve

**Scanning electron microscope**

The morphology of curcumin-NLC beads was characterized by a scanning electron microscope (SEM, LEO 1455 VP, Carl Zeiss, Oberkochen, Germany). Each sample was directly deposited on a carbon tape strip and subjected to gold sputter-coating before examining by SEM.

**Moisture content determination**

A moisture analyzer determined the moisture content (MA30 SARTORIUS, Göttingen, Germany). A 0.5 g of curcumin-NLC beads were placed on the moisture analyzer and heated at 130°C until the constant weight of the samples was obtained. The percentage of moisture content was calculated using Equation 7.

$$\textbf{Moisture content (\%)} = \frac{\textbf{initial weight-final weight}}{\textbf{initial weight}} \times 100 \quad \textbf{... (Equation 7)}$$

**Drug entrapment efficiency and percentage of drug loading**

The lyophilized curcumin-NLCs powder and curcumin-NLC beads were subjected to drug entrapment efficiency determination. Briefly, 20 mg of sample were dissolved in methanol and centrifuged at 18000 rpm for 30 min. The supernatant was then diluted with mobile phase, acetate buffer, and acetonitrile (50:50 (v/v)), pH 3.1, before being subjected to HPLC (Shimadzu Corporation, Japan). The HPLC was equipped with a Vertisep C18 column (5 µm, 4.6 x 250 mm), using a flow rate was 1.2 mL/min, and was detected by a UV detector at 423 nm. The curcumin concentration was quantified using a standard curve of 0.1 - 10.0 µg/mL. The percentage of curcumin entrapment and percentage of drug loading was calculated using Equation 8 and 9, respectively.

$$\textbf{Curcumin entrapment efficiency (\%)} = \frac{\textbf{Curcumin tested}}{\textbf{Curcumin initial}} \times 100 \quad \textbf{... (Equation 8)}$$

$$\textbf{Percentage of drug loading (\%)} = \frac{\textbf{weight of curcumin tested}}{\textbf{weight of NLC-beads}} \times 100 \quad \textbf{... (Equation 9)}$$

***In vitro* drug release study**

The release behaviors of the curcumin-NLCs and curcumin-NLC beads were investigated in 100 mL of simulated fluids at 37 ± 0.5°C under constant stirring at 80 rpm. The simulated fluids were fasted-state simulated gastric fluid (FaSSGF), pH 1.6, fasted state simulated intestinal fluid (FaSSIF), pH 6.5 and FaSSIF, pH 7.4 (90, 91). For the curcumin-NLCs, the sample was tested separately in FaSSGF for 2 h and in FaSSIF, pH 6.5, for 3 h and then adjusted to pH 7.4 for the remainder of the 12 h test period. Alternatively, curcumin-NLC beads were placed in FaSSGF for 2 h and

transferred to FaSSIF, pH 6.5, for 3 h before adjusting to pH 7.4, for the remainder of the 12 h test period. A 0.5 mL aliquot of each sample was withdrawn at time intervals and replaced with an equal amount of fresh medium. The released curcumin was determined by the HPLC method, with each experiment being conducted in triplicate

**Kinetics drug release and data analysis**

The curcumin release kinetics were determined using the software DDSolver program by fitting with five different kinetic models: the zero-order model, first-order model, the Higuchi model, Korsmeyer-Peppas kinetic model, and Hopfenberg kinetic model, as shown below(92).

Zero-order model:

$$M_t = M_0 + k_0 t$$

First-order model:

$$\log M_1 = \log M_0 + \frac{k_1 t}{2.303}$$

Higuchi model:

$$M_t = k_H \times t^{1/2}$$

Korsmeyer-Peppas model:

$$\frac{M_t}{M_{inf}} = kt^n$$

Hopfenberg:

$$\frac{M_t}{M_{inf}} = 1 - \left[1 - \frac{k_0 t}{C_0 a_0}\right]^n$$

where:

$M_t$ = the cumulative drug release at time t

$M_0$ = the initial amount of drug in the solution (most times, $M_0 = 0$)

$M_{inf}$ = the amount of drug released after time infinite

t = the release time

n = the release exponent, which indicates the drug release mechanism (table 7)

$C_0$= the initial concentration of drug in the matrix

$a_0$= the initial radius for a spherical particle

$k_0$, $k_1$, $k_H$ and k = the kinetic constant for zero order, first order, Higuchi and Korsmeyer- Peppas kinetic model, respectively.(93)

The best fit model was determined from the coefficient of determination (R2), the weighted sum of squares (WSS), Akaike information criterion (AIC), and model selection criterion (MSC), following the criteria as shown in Table 7.

**Table 7 Parameters for characterizing drug release kinetics model**

| Parameters | Interpretation to indicate a good fitting kinetic model |
|---|---|
| Coefficient of determination (R2) | Highest value (~1.0) |
| Standard deviation of residuals (WSS) | Lowest value |
| Akaike information criterion (AIC) | |
| Model selection criterion (MSC) | More than two to three |

**Stability study**

Curcumin-NLCs lyophilized powder and the curcumin-NLC beads were stored in a sealed amber glass bottle. Nitrogen gas was used to displace oxygen gas from the container to prevent oxidation. Then, both formulations were kept in darkness for 6 months at 4°C and at room temperature. The percentage of curcumin remaining was then calculated using the HPLC method.

**Statistical analysis**

All values were represented as the mean ± SD. Statistically significant differences between groups were determined by one-way analysis of variance (ANOVA) tests for statistical significance value, with $p < 0.05$.

# CHAPTER IV

# RESULTS AND DISCUSSION

This chapter presents the findings attained from the study, which includes the development of colon targeted oral delivery system, physicochemical characterization of curcumin-NLCs and curcumin NLC beads, *in vitro* release studies, kinetic release characterization, and stability of curcumin NLC beads.

**Preliminary study**

ES100 powders 1%, 3%, and 5%w/v can be dissolved by 0.2 M NaOH, whereas 10%w/v of ES100 was insoluble (Fig. 18). Therefore, the 1%, 3%, and 5%w/v of ES100 solutions were dropped in 1 M HCl while stirring at 100-600 rpm at room temperature, but the solution cannot form beads. For this reason, the ES100 beads were formulated without stirring. The 3% and 5% w/v of ES100 beads were stronger than 1%w/v of ES100, which were more fragile (Fig. 19). Before drying, the mean particle size of 3% and 5%w/v of ES100 was 2 mm. After drying, the mean particle size of 3% and 5%w/v of ES100 was less than 1 mm.

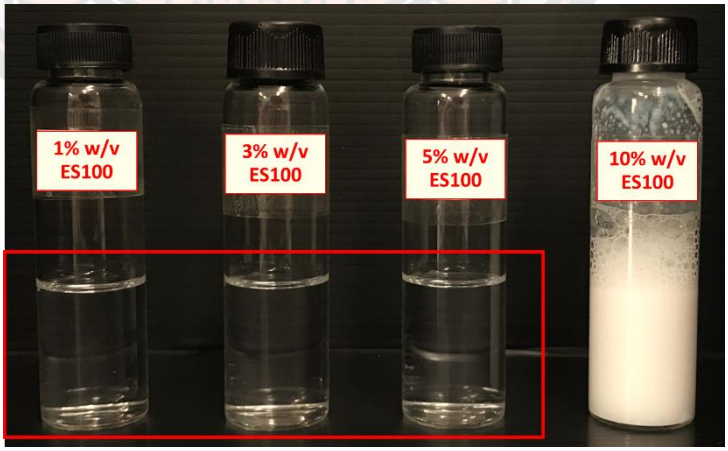


**Figure 18 Eudragit S100 solutions in 1%, 3%, 5% and 10% w/v concentration.**

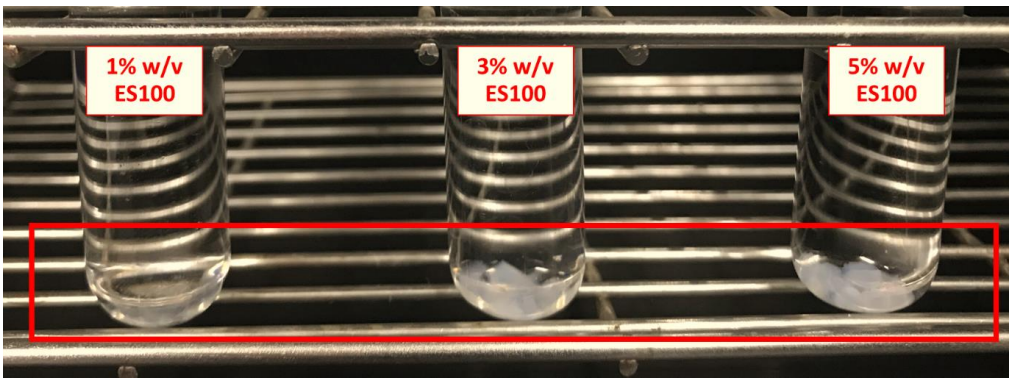


**Figure 19 Characterization of Eudragit S100 beads in 1%, 3% and 5% w/v concentration**

Therefore, the concentration of ES100 in a range of ≥3% w/v and <10% w/v was chosen. However, the solubility of ES 100 is a pH of more than 7.0, more than the pH of the proximal small intestine (pH 6.4). The ES100 beads may be insoluble in GI tract conditions; thus, EL 100-55, which is soluble at pH more than 5.5, was chosen for mixing with ES100 to develop desirable dissolved beads in GI tract conditions. Consequently, the ES100 and EL100-55 solutions were mixed in variance ratio and concentration (table 8). Moreover, $CaCl_2$ was chosen as a cross-linked agent that purposed readily bead formation by an intermolecular reaction between the divalent calcium ions and the negatively charged carboxyl group of Eudragit. Onwards, the ES100 and EL100-55 mixed solutions were dropped into the 5%, and 10% w/v of $CaCl_2$ in 1.0 N HCl solutions showed beads formation at 10-12% w/v of the total concentration of Eudragit. After the beads were dried, these beads were investigated for dissolution properties in the 1.0 N HCl pH 1.2 and PBS buffer pH 6.8. However, the mixing Eudragit beads dissolved in pH 1.2 for 2 h. and pH 6.8 within 1 h., which may early release the active agent before reaching the colon.

**Table 8 Dissolution test of ES100 and EL100-55 particles with HCl pH 1.2 and Phosphate buffer pH 6.8**

| ES100% (w/v) | EL100-55% (w/v) | $CaCl_2$ %(w/v) | Dissolution time(hour) | |
|---|---|---|---|---|
| | | | pH 1.2 | pH 6.8 |
| 3 | 7 | 5 | 2 | 1 |
| 3 | 7 | 10 | 2 | 1 |
| 5 | 5 | 5 | 2 | 1 |
| 5 | 5 | 10 | 2 | 1 |
| 5 | 7 | 5 | 2 | 1 |
| 5 | 7 | 10 | 2 | 1 |

As a result, the only ES 100 bead was focused again but varied the concentration. Therefore, the ES100 beads were prepared using Eudragit S100 in a concentration of 1-9% w/v and dropped into the 10% w/v of $CaCl_2$ in 1.0 N HCl solution. After preparation, the ≤ 3% w/v of Eudragit S100 cannot form the bead. Afterward, 5%, 7%, and 9% w/v of ES100 beads were dissolution examined to find the suitable concentration of ES beads for colon targeted drug delivery system. The results demonstrate that 5%w/v ES100 beads eroded in the acid condition. On the contrary, the 9% w/v and 7%w/v ES100 beads were not eroded even after 24 h of soaking time in PBS pH 6.8 condition.

**Table 9 the preliminary studies result of bead formation and dissolution time of variance concentration of ES100 (ND= No determined)**

| ES100 (%w/v) | Bead formation | Dissolution time in 0.1 N HCl pH 1.2 (hour) | Dissolution time in phosphate buffer pH 6.8 (hour) |
|---|---|---|---|
| 1 | No bead formation | ND | ND |
| 3 | No bead formation | ND | ND |
| 5 | Irregular shape | 2 | 1 |
| 7 | Spherical shape | >24 | >4 |
| 9 | Spherical shape | >24 | >4 |

To the above results, the Eudragit mixed beads showed faster dissolution than 7% and 9% w/v ES100 due to the solubility of EL100-55 soluble at pH>5.5. Therefore, the dissolution of EL100-55 led to pore formation inside the beads, then increased the surface area, resulting in faster solubilization, even though the total amount of mixed Eudragit beads were more than ES100 beads. Consequently, 7% and 9% ES100 beads were chosen to develop for colon-targeted oral drug delivery system.

**High-performance liquid chromatography (HPLC) analysis for curcumin**

The standard curcumin was analyzed by the reverse-phase method of HPLC at wavelength 423 nm. The calibration curve of curcumin in the range of 0.1-10.0 µg/ml was constructed by its absorbance values versus the curcumin concentrations as shown in the figure. 20. The calibration curve equation was $y = 100566x - 4213.2$ ($R^2 = 0.9999$)

**Table 10 Peak area of standard curcumin determined by HPLC**

| Concentration of curcumin (µg/ml) | Peak area at 423 nm | | | | |
|---|---|---|---|---|---|
| | 1 | 2 | 3 | Mean | SD |
| 0.1 | 10074 | 9979 | 10358 | 10137 | 160 |
| 0.5 | 51696 | 52012 | 47554 | 50420 | 2031 |
| 1 | 84127 | 96168 | 95037 | 90899 | 5429 |
| 2 | 191317 | 202831 | 193625 | 195924 | 4973 |
| 4 | 366073 | 426065 | 397071 | 396403 | 24495 |
| 6 | 592051 | 620933 | 583690 | 598891 | 15955 |
| 8 | 763962 | 847563 | 774916 | 795480 | 37098 |
| 10 | 951720 | 1048923 | 1019373 | 1006672 | 40686 |

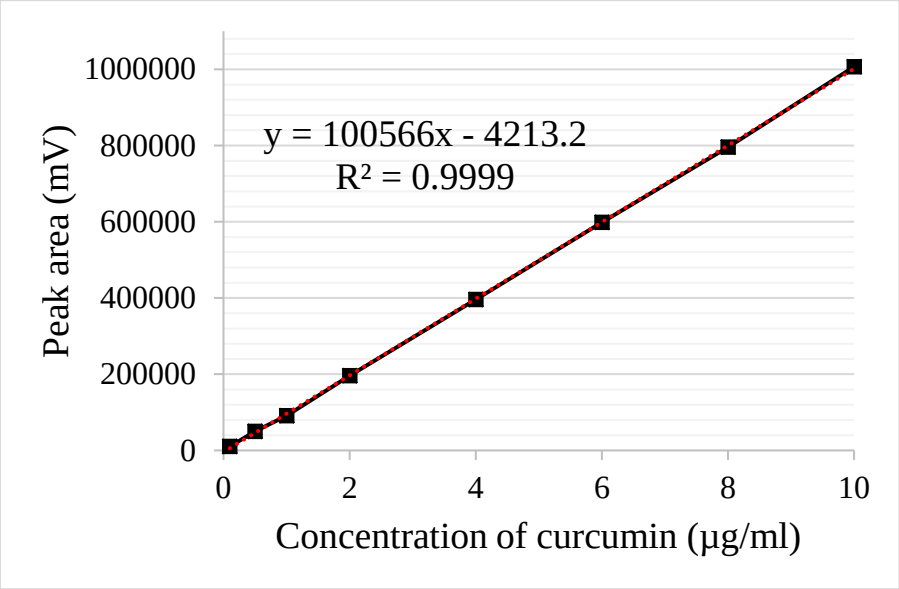


**Figure 20 Calibration curve of standard curcumin by HPLC at 423 nm**

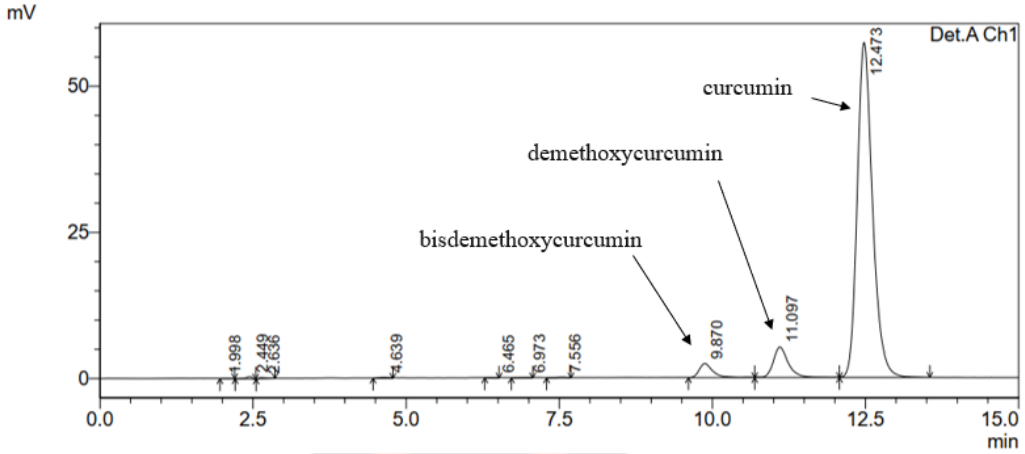


**Figure 21 The HPLC chromatogram of standard curcumin at 423 nm**

**Physicochemical characterization of curcumin-NLCs**

Curcumin-NLCs were successfully prepared using a warm microemulsion technique. The mean particles size and size distribution were determined by dynamic light scattering with a ZetaPALS® analyzer. The curcumin-NLCs exhibited a mean size of 227.75±0.71 nm. The PI value was less than 0.3, which indicated a narrow size distribution. The prepared NLC manifested negatively charged with a zeta potential of -55.96 ± 1.88 mV, and the drug loading percentage was 0.28±0.02% with a high curcumin entrapment efficiency of ~90%. The nanosized would render them able to adhere to the target site and allow for prolonged drug action. In addition, by incorporating the drug in the lipid matrix, the chemical stability of the drug during storage and passage through the GIT could be improved.

**Physicochemical characterization of curcumin-NLC beads**

The curcumin-NLCs beads were prepared by using the ionotropic gelation technique based on electrostatic interactions. The beads were formed as a result of the ionic reaction that occurred between the anions of the Eudragit S100 polymer and a cationic ($Ca^{2+}$) as a cross-linking agent. When Eudragit S100 was dissolved in 2.0 N NaOH solution, the hydrogen atom separated from carboxylic groups, forming -COO- groups. The COO- from the Eudragit S100 and $Ca^{2+}$ from $CaCl_2$ interact through intermolecular electrostatic interactions, giving rise to a water-insoluble precipitates as a spherical bead(79, 94).

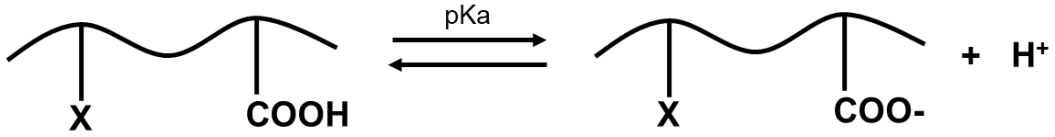


**Figure 22 The ionization of Eudragit S100's carboxylic group**

**Mean size and morphology of the beads**

The mean bead size, determined by the sieving method, was 0.993 ± 0.001 mm for the 7ES and 1.041 ± 0.011 mm for the 9ES, with a narrow size distribution in the range of 0.6 to 1.6 mm.

The increase in the polymer concentration leads to a gradual increase in bead size. This phenomenon can be explained based on the viscosity of the EudragitS100 solution. The increasing polymer concentration usually accompanies the increasing viscosity of the polymer solution. As a result, the droplet is formed bigger leading to a bigger ES bead size. The control of bead sizes by changing polymer concentrations. It was explained that the increase in polymer concentration leads to an increase in the viscous forces resisting the solution to be separated into droplets, leading to an increase in particle size(95, 96).

The appearance of the curcumin-NLC beads under an optical microscope showed a light yellowish spherical shape (Fig. 23). After drying, the surface and internal structure of the curcumin-NLC beads were examined using SEM. Both formulations illustrated a rough surface, while the cross-sectional structure illustrated a smoother and more densely packed structure. Nevertheless, the surface and cross-sectional profile of the 7ES beads showed more porosity than 9ES (Fig. 24). The curcumin-NLCs were found to be evenly distributed in the polymer matrix.

The curcumin-NLCs were further entrapped in a pH-sensitive bead employing ES, pKa of 6, as a bead carrier. The beads were simply produced by the ionotropic gelation technique. The beads were formed spontaneously via ionic interaction between the carboxylic group of the ES and calcium as a cross-linking agent, resulting in a water-insoluble salt precipitated as a spherical rigid bead(79, 94). The preparation method is

simple, and the mean size was approximately 1 mm, which depends on the dropper size. Curcumin-NLCs were found evenly distributed in the polymer matrix, confirmed by SEM (Fig 24c, f).

Similar to particle size, the morphology result revealed that the level of porosity of beads was dependent on the concentration of polymer in the formulation. The high content of Eudragit takes leads to a decrease in porosity. The surface morphology of the beads was dependent on the concentration of Eudragit polymer solution. Since the proton($H^+$) and free $Ca^{2+}$ rapid bound with the Eudragit solution molecule leads to separation from the aqueous phase, forming a viscous droplet in the HCl solution, resulting in low water inside the bead. This phenomenon is rapid in a higher concentration of polymer solution. Therefore, with a decrease in concentration, the surface became rough and porous. At higher Eudragit concentration, a smooth surface with low porosity was formed on the surface of the beads(96, 97).

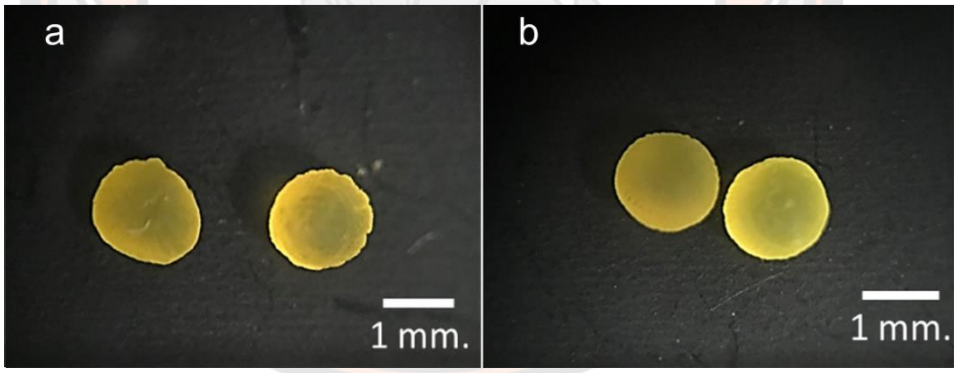


**Figure 23 Optical micrographs of curcumin-NLCS beads; (a) 7ES, and (b) 9ES. The beads showed a spherical shape with light yellow color.**

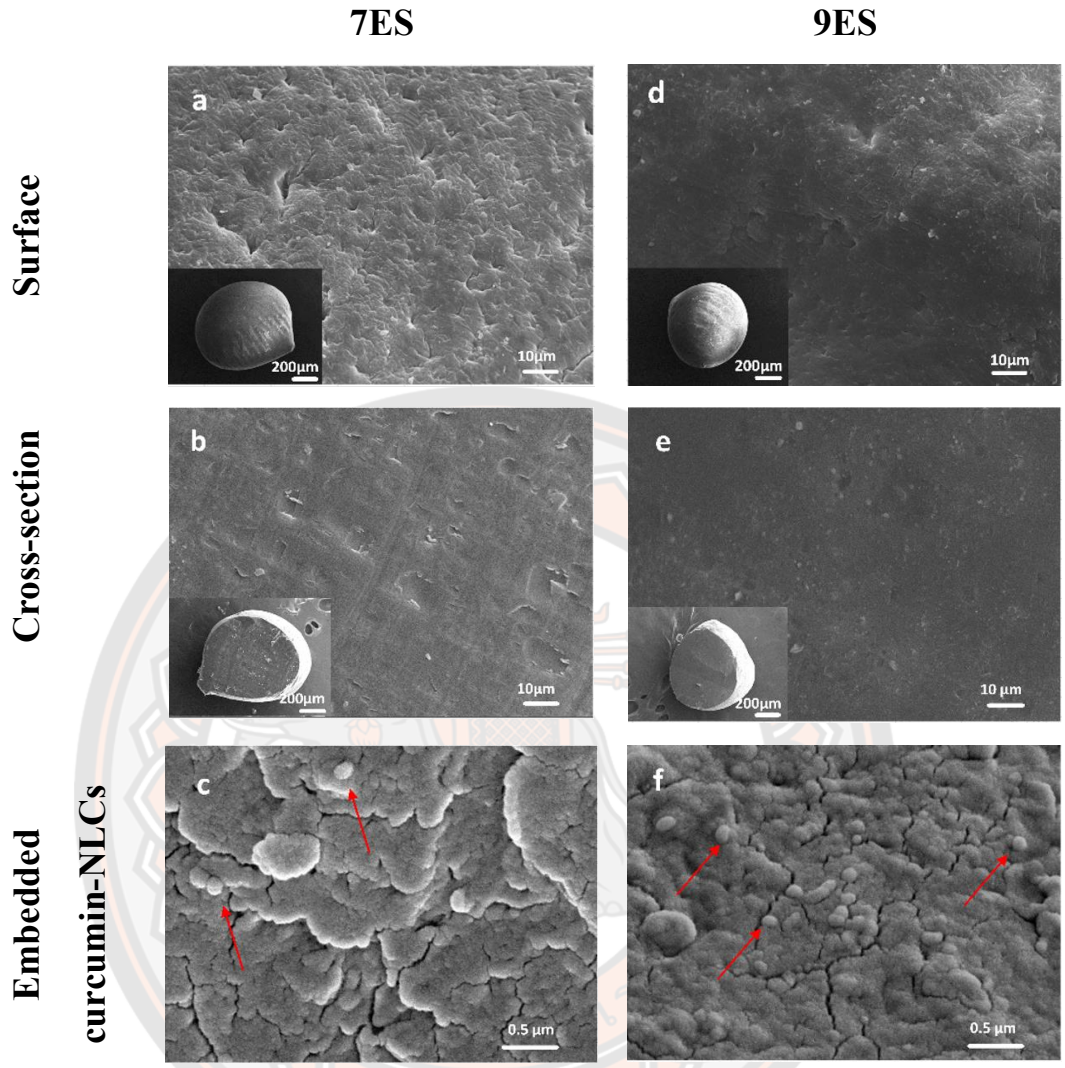


**Figure 24 Morphology of curcumin-NLCS beads; SEM micrographs of surface (a,d), cross-section (b,e), and embedded curcumin-NLCs (c,f) of 7ES beads (a-c), and 9ES beads (d-f). The red arrows indicated embedded curcumin-NLCs in the polymer matrix.**

**Entrapment efficacy and percent drug loading of curcumin-NLC beads**

The percent drug loading of 7ES and the 9ES beads showed 0.14±0.02% and 0.10±0.00%, respectively. In addition, both of the 7ES and the 9ES beads indicated a high curcumin entrapment efficiency of 81.01±5.24% for the 7ES, with a moisture content of 3.54±0.18%, and 92.75±6.02% for the 9ES beads, with a moisture content of 1.45±0.15%. Similar to size and morphology of the beads, entrapment efficacy was dependent on the composition of the beads as well as Eudragit (98). Low content of Eudragit in formulation resulted with low entrapment of drug in bead formulations. Under the influence of polymer concentration, a high concentration increases the viscosity of the solution leading to a rise in droplet-separated resist and then rapid bead forming. For this reason, the curcumin-NLC leakage while the rapid bead forming process was decreased, resulting in a percentage of entrapment of 9ES is significantly higher than 7ES.

***In vitro* drug release studies**

The curcumin-NLCs exhibited a burst release characteristic in both FaSSGF and FaSSIF conditions; 54.49±6.12% within 1$^{st}$ h for the FaSSGF and 53.50±8.41% within 30 min for the FaSSIF, as shown in Figure 25. These results suggest that curcumin-NLCs showed early drug release before reaching the target site (colon; FaSSIF pH 7.4 condition). As known, the advantage of NLCs is solubility enhancement owing to the surface area increased by the nanoscale size of the particles. In this case, these results suggest that curcumin-NLCs showed early drug release before reaching the target site (colon; FaSSIF pH 7.4 condition), an undesirable outcome for the targeted drug delivery system. However, the solubility enhancement property of NLCs still is needed for low solubility drugs such as curcumin.

On the other hand, both curcumin-NLC beads, 7ES and 9ES, could prevent the curcumin released in gastric condition as no curcumin was detected in FaSSGF after 2 h incubation. However, in FaSSIF (pH 6.5), 30% curcumin was gradually released from the beads. Then, after adjusting the FaSSIF to pH 7.4, the beads showed sustained release characteristics, with 95% of the curcumin being released within 12 h (Fig. 26a).

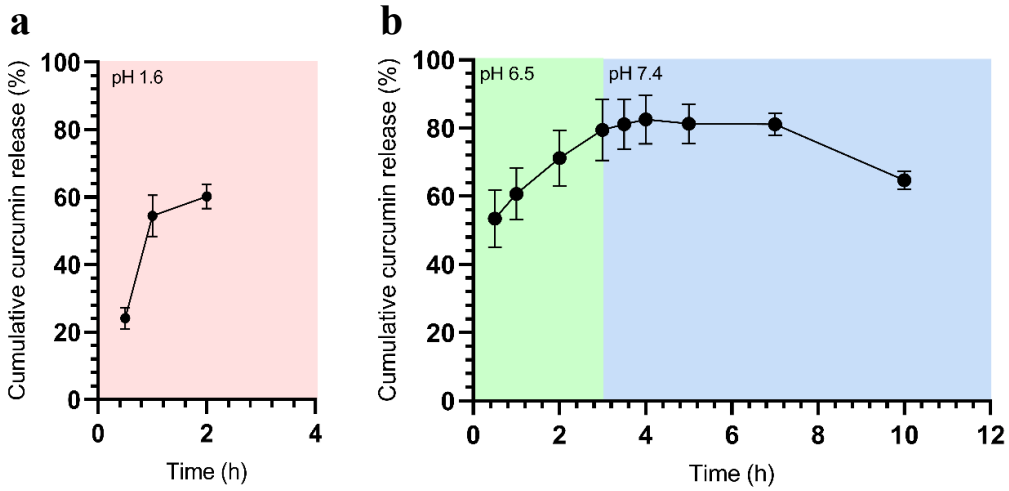


**Figure 25 In vitro dissolution profile of curcumin-NLCs in (a) FaSSGF pH 1.6, and (b) FaSSIF pH 6.5 and 7.4. Data is represented as mean ± SD (n = 3).**

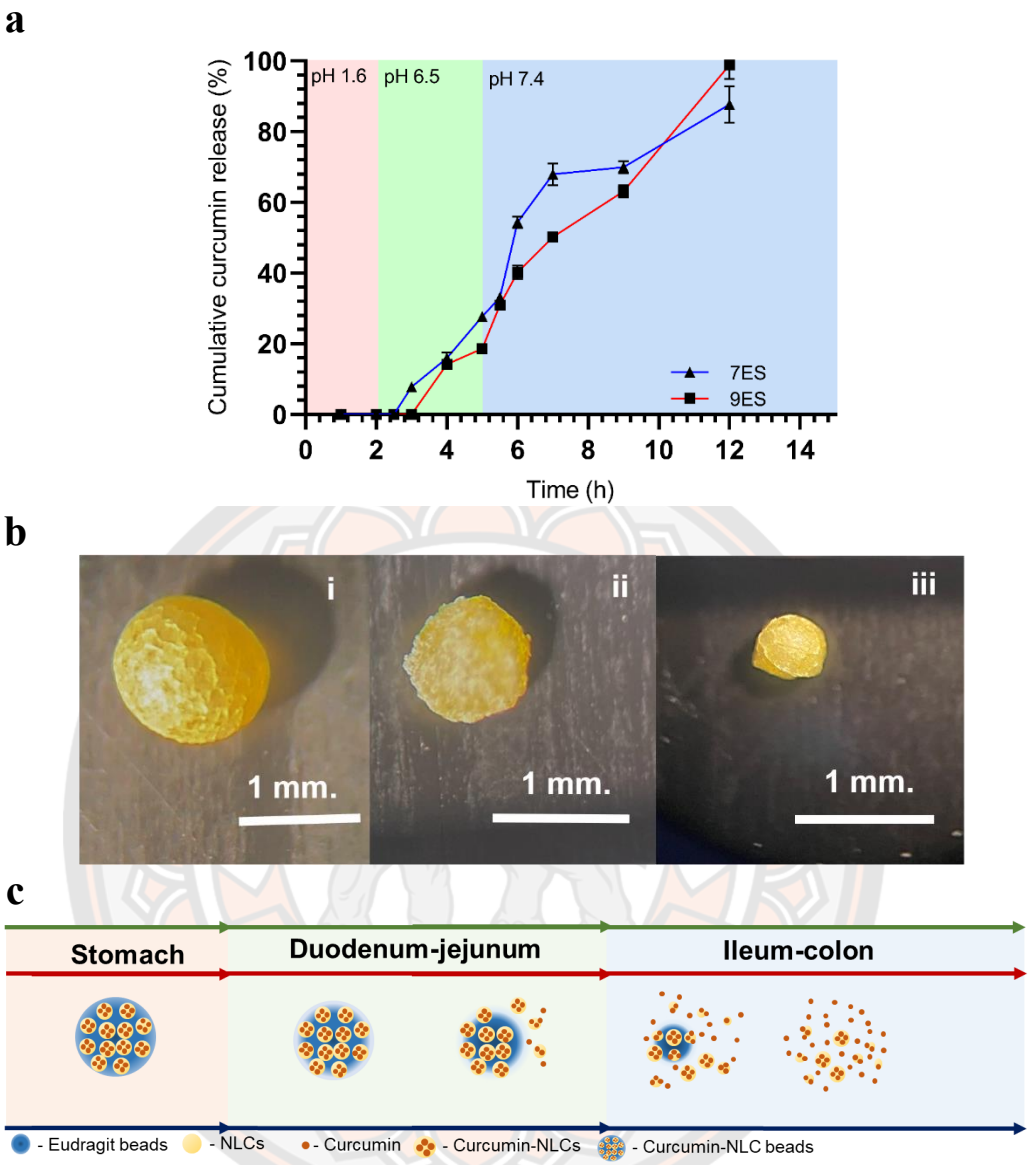


**Figure 26 (a) In vitro dissolution profile of curcumin-NLCS beads; 7ES and 9ES, in different dissolution medium pH to mimic drug release from the stomach to the colon. Data is represented as mean ± SD (n = 3). (b) Optical micrographs of curcumin-NLC beads from release study; (i) 2h in FaSSGF pH 1.6, (ii) 3h in FaSSIF pH 6.5, and (iii) 4h in FaSSIF pH 7.4. The beads showed size reduction in the time course of the experiment, which indicated surface erosion. (c) Schematic illustration of proposed drug release from NLCS-beads in different dissolution medium pH. Intact curcumin-NLCS beads presented in FaSSGF, some bead erosion occurred in FaSSIF pH 6.5 resulting in small amount of curcumin release, and bead erosion presented in FaSSIF pH 7.4 resulting in more curcumin released.**

To elucidate the release mechanism, the release data were fitted to the zero-order model, first-order model, Higuchi model, Korsmeyer-Peppas model, and the Hopfenberg model. The best fit kinetic model was then determined and evaluated using 4 statistical parameters: $R^2$, WSS, MSC and AIC. The maximum value of $R^2$ and MSC, and minimum value of WSS and AIC indicated the best-fitted kinetic model. Both 7ES and 9ES were fitted to a zero-order model with $R^2$ of 0.9049 and 0.9545, respectively. The release mechanism followed an Hopfenberg model, with $R^2 > 0.95$, meaning that drug release was enabled through surface erosion of the polymer matrix. Following the Korsmeyer-Peppas model, 7ES and 9ES showed $R^2$ of > 0.93 with dissolution exponent (n) of 1.883 and 1.615, respectively (Table 6) indicating that dissolution occurs through the case II transport mechanism. Furthermore, optical micrographs showed the bead size remained intact after being incubated in FaSSGF at pH 1.6 for 2 h, while after being incubated in FaSSIF, pH 6.8, and pH 7.4, the size of the beads showed gradually decreased with time, beginning from the surface (Fig 26b). Thus, the mechanism of drug release from curcumin-NLC beads has been proposed in Fig 26c.

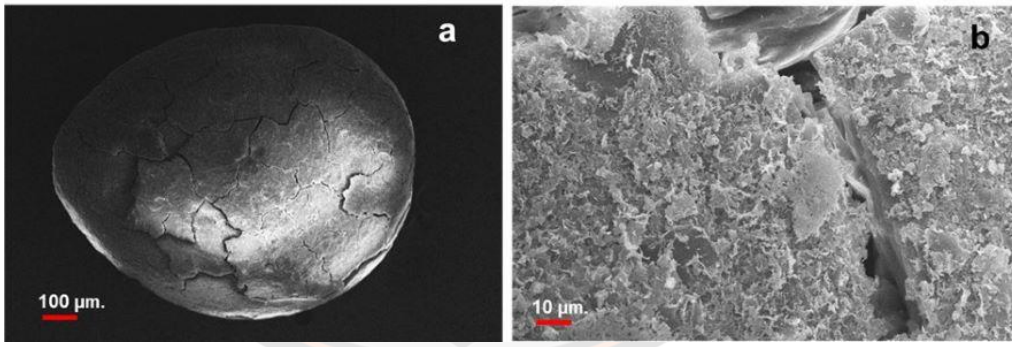


**Figure 27 Morphology of curcumin-NLC beads; SEM micrographs from release study in 3h at FaSSIF pH 6.5 of the curcumin-NLC bead (a), and cross surface (b) indicated the surface erosion while releasing of the drug.**

As the results, the combination of NLCs and pH-sensitive beads could prevent early drug release in the upper GIT. Furthermore, a sustained released characteristic in the small intestine and colon was achieved within 12 h. The release mechanism of NLC-beads has been proposed in Fig 26c. In gastric conditions, the intact beads were observed to have no curcumin release. This is because ES is insoluble in an acidic medium. Nevertheless, when the beads were transferred to the medium pH 6.5, which is greater than the pKa of ES, the polymer dissolution was triggered(10, 77). Consequently, the bead surface erosion occurred resulting in curcumin-NLCs leaking out to the dissolution medium, and gradually releasing curcumin from the NLCs as a function of time. In FaSSIF, pH 7.4, representing distal small intestine and colon conditions, the polymer erosion was continued until the bead completely dissolved and a complete curcumin release was observed within 12 h. The release mechanism of NLC-beads was fitted with Hopfenberg and Korsmeyer-Peppas model, with an $R^2$ value greater than 0.9. Basically, the Hopfenberg model suggested drug release through surface-erosion of matrix (88, 99, 100), which could maintain the effective drug concentration and prevent dose dump leading to minimize dose frequency administration and toxicity (101, 102). Similarly, the diffusion coefficient, n value, obtained from the Korsmeyer-Peppas model also was > 0.85, indicating case II transport which the drug release mechanism associated with polymer disentanglement and erosion (81, 93, 103). Therefore, the main drug release mechanism of 7ES and 9ES beads is surface erosion of the matrix. In addition, the drug release kinetics was also fitted with zero-order, indicating this system could release the drug at a constant rate and independent of drug concentration(104).

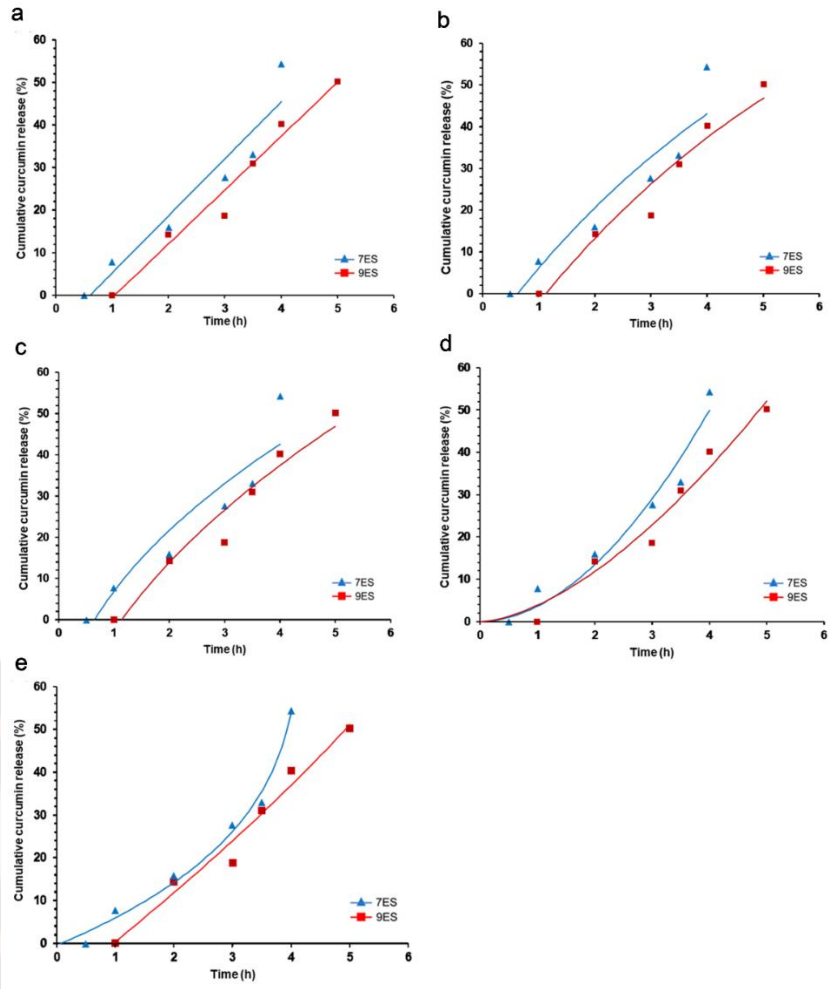


**Figure 28 Drug release profile of curcumin-NLCs beads fitted with different kinetic model; (a) zero order, (b) first order, (c) Higuchi, (d) Korsmeyer-pappas, and (e) Hopfenberg. The symbol is represented as mean ± SD (n = 3), and line is represented the predicted**

In addition, the drug release rate was affected by polymer concentration. From the *in vitro* drug release profiles, the higher ES concentration beads, 9ES, showed a trend of slower released rate than the lower one, 7ES. The reduction in drug release rate can be explained by the slow hydrolysis of the matrix. As the amount of polymer increased, the less porous structure was obtained, as evidenced from the bead morphology (Fig 24a, d), which led to retard polymer erosion process (97, 98, 105).

Upon curcumin-NLCs was released from the pH-sensitive beads, the nano-size allowed them to adhere well at the target sites which should prolong local drug availability and permit a reduction in dosing frequency (106, 107). Additionally, their negatively charged surface offers a synergistic benefit for IBD treatment. Generally, the inflammation of the colonic mucosa is accompanied by the mucus layer depletion and in situ accumulation of positively charged proteins including transferrin (108). Thus, a damaged epithelial surface with a positive charge would provide a binding affinity with negatively charged drug carriers. As a result, this combination has a possibility to the specific colon delivery system by oral administration, especially for IBD.

However, one advantage of NLCs is increased water solubility of a poorly water-soluble substance. Accordingly, NLCs could not protect the curcumin dissolution in the upper GIT. As evident from in vitro drug release studies, curcumin-NLCs exhibited a burst drug release of > 50% in 1 h at both FaSSGF and FaSSIF conditions. Curcumin is notorious for its instability due to hydrolysis and oxidation (27, 50, 109). Therefore, NLCs cannot protect curcumin degradation in the upper GIT owing to early drug release.

**Table 11 Estimated parameters, coefficient of determination ($R^2$), weighted sum of squares (WSS), Akaike information criterion (AIC), and model selection criterion (MSC), obtained from fitting experimental data of curcumin-NLCS beads to different kinetic models.**

| **7ES beads** | **$R^2$** | **WSS** | **AIC** | **MSC** | |
|---|---|---|---|---|---|
| **Zero-order** | 0.9049 | 145.9052 | 33.8977 | 1.5809 | |
| **First-order** | 0.8658 | 205.7906 | 35.9612 | 1.2370 | |
| **Higuchi** | 0.8457 | 236.6403 | 36.7992 | 1.0973 | |
| **Korsmeyer-Peppas** | 0.9320 | 78.1677 | 32.1531 | 1.8717 | n = 1.883 |
| **Hopfenberg** | 0.9815 | 21.2710 | 24.3441 | 3.1732 | |
| **9ES beads** | **$R^2$** | **WSS** | **AIC** | **MSC** | |
| **Zero-order** | 0.9630 | 49.7615 | 27.4435 | 2.3532 | |
| **First-order** | 0.9371 | 84.4951 | 30.6202 | 1.8238 | |
| **Higuchi** | 0.9316 | 91.9099 | 31.1249 | 1.7397 | |
| **Korsmeyer-Peppas** | 0.9411 | 59.3622 | 30.5025 | 1.8434 | n = 1.615 |
| **Hopfenberg** | 0.9545 | 45.8540 | 28.9528 | 2.1017 | |

n = The release exponent interpretation of the Kormeryer-pappas releasing model from spherical shape particles; n = 0.43 indicates Fickian diffusion, $0.43<n<0.85$ indicates Anomalous transport, and $n \geq 0.85$ indicates Case II transport.

**Stability**

The lyophilized curcumin-NLCs showed good curcumin stability during the 6-month storage at both 4°C and room temperature, with > 90% curcumin remaining. On the contrary, after 6-month storage at room temperature, 7ES and 9ES beads exhibited curcumin degradation, which decreased the curcumin remaining in the 7ES beads to 32.90±5.46% and to 64.48±8.05% in the 9ES beads. Nevertheless, both 7ES and 9ES beads stored at 4°C showed greater curcumin chemical stability with > 95% curcumin remaining after 3-month storage which decreased to ~90% after 6-month storage with no statistically significant difference (Fig.29).

Curcumin is notorious for its instability. Thus, the chemical stability of curcumin in both lyophilized NLCs and beads was observed. The lyophilized curcumin-NLCs showed good curcumin stability during 6-month storage at both 4°C and room temperature, > 90% curcumin remaining. However, both curcumin-NLC beads revealed curcumin degradation after 6-month storage at room temperature. The percentage of curcumin remaining of 7ES and 9ES were 30 and 65, respectively. It is worth noting that the moisture content of 7ES was 3.54 ± 0.18% and of 9ES was 1.45 ± 0.15%, which results in a tendency to the faster curcumin degradation observed in 7ES than that in 9ES. Therefore, the curcumin degradation during storage at room temperature was a result of the hydrolysis reaction, which was accelerated by the moisture content in the bead and elevated temperature(50, 109). Nevertheless, the curcumin stability could be maintained by storage at 4°C, as both formulations showed ~ 90% curcumin remaining.

**a**

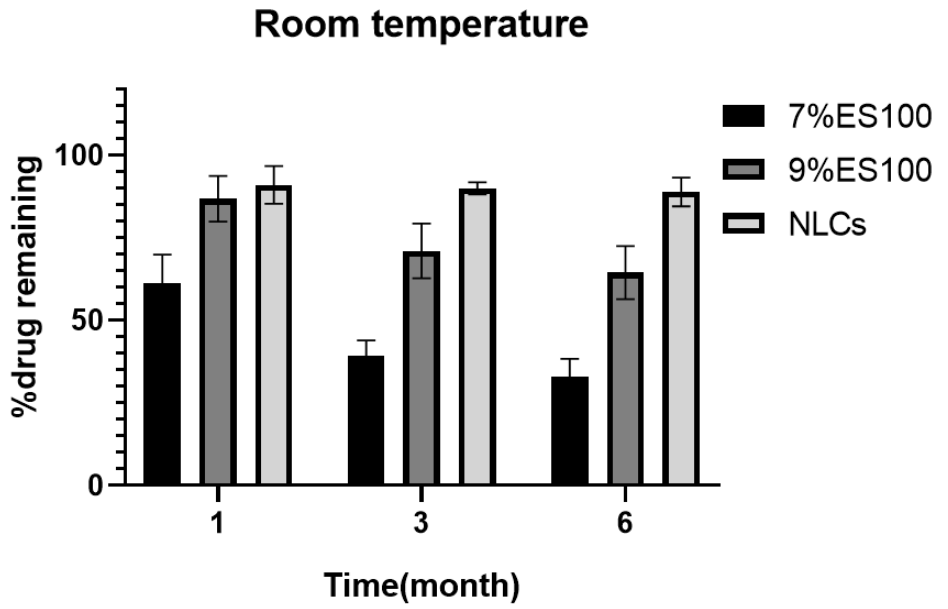


**b**

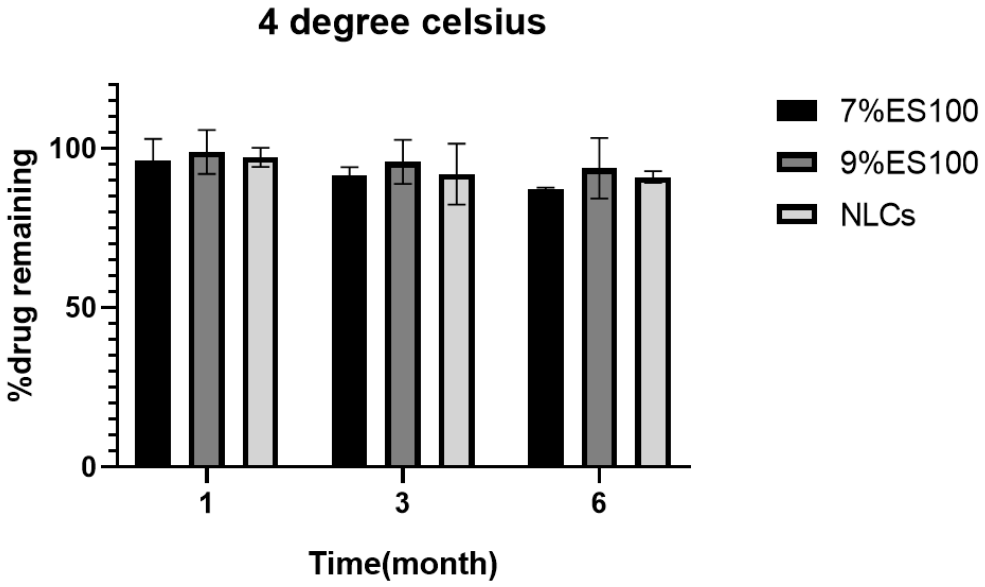


**Figure 29 The percentage of curcumin remaining after 6-month storage in the absence of light at (a) room temperature, and (b) 4°C. Data is represented as mean ± SD (n=3).**

# CHAPTER V

# CONCLUSION

Colon-targeted drug delivery is an active area of research for local colon diseases, including inflammatory bowel disease (IBD). It could improve the therapeutic efficacy and reduce local and dose-dependent systemic toxicity. The oral route is generally the most desirable and acceptable route, but it is limited by drug loss due to early drugs released in the upper GIT. Therefore, to develop the colon-targeted drug delivery system via oral administration, the formulation must resist drug dissolution under gastric pH conditions and release the drug upon alkaline pH in the small intestine. To achieve the above, an orally colon-targeted drug delivery system has been developed using a combination of nanoparticles in pH-sensitive beads. Curcumin, an anti-inflammatory agent, has been used as a model drug owing to this compound being unstable in alkaline conditions.

In this study, the combination system of curcumin-NLCs entrapped in pH-sensitive beads (curcumin-NLC beads) for an orally colon-targeted drug delivery system was successfully developed. To be orally administered and localized to the colon, the NLCs in beads could remain intact in the upper GIT and, thus, prevent early drug dissolution and drug degradation. As a result, the only curcumin-NLCs exhibited early drug release in both acidic and alkaline conditions. In this study, the dissolution of the beads was triggered by alkaline pH in the ileocolonic region, resulting in curcumin-NLCs leaking out from the beads. Therefore, Eudragit S100 (ES100), a pH-sensitive polymer with a solubility threshold higher than pH 7.0, was exploited. The preparation of curcumin-NLC beads has successfully promoted light yellowish spherical beads and entrapped curcumin-NLCs inside the bead matrix via mixing the curcumin-NLCs dispersion with ES100 solution then dropping them into an acidic medium. In the ionotropic gelation techniques, the bead formation process under acidic conditions couples the negative charge of ES100 and the positive charge of the proton($H^+$). At the same time, calcium ions, cross-linkage agents, enhanced rigidify of the beads.

Moreover, the curcumin-NLC beads showed a high entrapped efficacy about 80%. After six months of storage at 4 degrees Celsius, curcumin-NLC beads exhibited good stability, with 90% of the curcumin drug remaining. *In vitro* release study, the curcumin-NLC beads revealed sustained drug release of up to 12 h was obtained. The released kinetics was fitted with Hopfenberg and a zero-order model, indicating this system could deliver the drug to the colon at a controlled and constant rate. In addition, NLCs could offer prolonged residence time at the target site that could benefit from reducing drug administration frequency along with its dose-related side effects. In conclusion, the developed pH-sensitive bead containing drug-loaded NLCs showed high potential for delivering drugs specifically to the colon by oral administration.

However, further studies are required to investigate curcumin-NLC beads *in vivo* study. Optimistically, it can be the colon specific-site drug delivery carrier via the oral route, which is possible to undertake the switch to large-scale production and marketing of the final product.

# REFERENCES

1. Vecchi Brumatti L, Marcuzzi A, Tricarico PM, Zanin V, Girardelli M, Bianco AM. Curcumin and inflammatory bowel disease: potential and limits of innovative treatments. Molecules. 2014;19(12):21127-53.
2. Nakase H, Uchino M, Shinzaki S, Matsuura M, Matsuoka K, Kobayashi T, et al. Evidence-based clinical practice guidelines for inflammatory bowel disease 2020. J Gastroenterol. 2021;56(6):489-526.
3. Testa A, Castiglione F, Nardone OM, Colombo GL. Adherence in ulcerative colitis: an overview. Patient Prefer Adherence. 2017;11:297-303.
4. Gavhane YN, Yadav AV. Loss of orally administered drugs in GI tract. Saudi Pharm J. 2012;20(4):331-44.
5. Stallmach A, Hagel S, Bruns T. Adverse effects of biologics used for treating IBD. Best Pract Res Clin Gastroenterol. 2010;24(2):167-82.
6. Zeeshan M, Ali H, Khan S, Khan SA, Weigmann B. Advances in orally-delivered pH-sensitive nanocarrier systems; an optimistic approach for the treatment of inflammatory bowel disease. Int J Pharm. 2019;558:201-14.
7. Liu L, Yao W, Rao Y, Lu X, Gao J. pH-Responsive carriers for oral drug delivery: challenges and opportunities of current platforms. Drug Deliv. 2017;24(1):569-81.
8. Franco FCZ, Oliveira MCC, Gaburri PD, Franco DCZ, Chebli JMF. High Prevalence of Non-Adherence to Ulcerative Colitis Therapy in Remission: Knowing the Problem to Prevent Loss. Arq Gastroenterol. 2022;59(1):40-6.
9. Ofridam F, Tarhini M, Lebaz N, Gagnière É, Mangin D, Elaissari A. pH-sensitive polymers: Classfication and some fine potential applications. Polymers for Advanced Technologies. 2021;32(4):1455-84.
10. Wang XQ, Zhang Q. pH-sensitive polymeric nanoparticles to improve oral bioavailability of peptide/protein drugs and poorly water-soluble drugs. Eur J Pharm Biopharm. 2012;82(2):219-29.
11. Ghaffar A, Yameen B, Latif M, Malik MI. pH-sensitive drug delivery systems. Metal Nanoparticles for Drug Delivery and Diagnostic Applications2020. p. 259-78.
12. Maurer AH. Gastrointestinal Motility, Part 1: Esophageal Transit and Gastric Emptying. Journal of Nuclear Medicine Technology. 2016;44(1):1-11.
13. Maurer AH. Gastrointestinal Motility, Part 2: Small-Bowel and Colon Transit. Journal of Nuclear Medicine Technology. 2016;44(1):12-8.
14. Pinto JF. Site-specific drug delivery systems within the gastro-intestinal tract: from the mouth to the colon. Int J Pharm. 2010;395(1-2):44-52.
15. Reyes-Ortega F. pH-responsive polymers: properties, synthesis and applications. Smart Polymers and their Applications2014. p. 45-92.
16. Khatik R, Mishra R, Verma A, Dwivedi P, Kumar V, Gupta V, et al. Colon-specific delivery of curcumin by exploiting Eudragit-decorated chitosan nanoparticles in vitro and in vivo. Journal of Nanoparticle Research. 2013;15(9).
17. Thakral S, Thakral NK, Majumdar DK. Eudragit®: a technology evaluation. Expert Opinion on Drug Delivery. 2013;10(1):19.
18. Franco P, De Marco I. Eudragit: A Novel Carrier for Controlled Drug Delivery in Supercritical Antisolvent Coprecipitation. Polymers (Basel). 2020;12(1).
19. Patra CN, Priya R, Swain S, Kumar Jena G, Panigrahi KC, Ghose D. Pharmaceutical significance of Eudragit: A review. Future Journal of Pharmaceutical Sciences. 2017;3(1):33-45.

20. Sonje A, Chandra A. Comprehensive Review on Eudragit Polymers. International Research Journal of Pharmacy. 2013;4(5):71-4.
21. El-Maghawry E, Tadros MI, Elkheshen SA, Abd-Elbary A. Eudragit-S100 Coated PLGA Nanoparticles for Colon Targeting of Etoricoxib: Optimization and Pharmacokinetic Assessments in Healthy Human Volunteers. Int J Nanomedicine. 2020;15:3965-80.
22. Fang M, Jin Y, Bao W, Gao H, Xu M, Wang D, et al. In vitro characterization and in vivo evaluation of nanostructured lipid curcumin carriers for intragastric administration. Int J Nanomedicine. 2012;7:5395-404.
23. Poonia N, Kharb R, Lather V, Pandita D. Nanostructured lipid carriers: versatile oral delivery vehicle. Future Science OA. 2016;2(3).
24. Zhu J. Curcumin and Its oxidative degradation products Their comparative effects on inflammation: University of Massachusetts Amherst; 2016.
25. Taylor RA, Leonard MC. Curcumin for inflammatory bowel disease: a review of human studies. Alternative medicine review : a journal of clinical therapeutic. 2011;16(2):152-6.
26. Heger M, van Golen RF, Broekgaarden M, Michel MC. The molecular basis for the pharmacokinetics and pharmacodynamics of curcumin and its metabolites in relation to cancer. Pharmacol Rev. 2014;66(1):222-307.
27. Kharat M, Du Z, Zhang G, McClements DJ. Physical and Chemical Stability of Curcumin in Aqueous Solutions and Emulsions: Impact of pH, Temperature, and Molecular Environment. J Agric Food Chem. 2017;65(8):1525-32.
28. Ordás I, Eckmann L, Talamini M, Baumgart DC, Sandborn WJ. Ulcerative colitis. The Lancet. 2012;380(9853):1606-19.
29. Torres J, Mehandru S, Colombel J-F, Peyrin-Biroulet L. Crohn's disease. The Lancet. 2017;389(10080):1741-55.
30. Torres EA. Inflammatory bowel disease (IBD). American Gastroenterological Association2022.
31. Ungaro R, Mehandru S, Allen PB, Peyrin-Biroulet L, Colombel J-F. Ulcerative colitis. The Lancet. 2017;389(10080):1756-70.
32. Riansuwan W, Limsrivilai J. Current status of IBD and surgery of Crohn's disease in Thailand. Ann Gastroenterol Surg. 2021;5(5):597-603.
33. Raine T, Bonovas S, Burisch J, Kucharzik T, Adamina M, Annese V, et al. ECCO Guidelines on Therapeutics in Ulcerative Colitis: Medical Treatment. J Crohns Colitis. 2022;16(1):2-17.
34. Rubin DT, Ananthakrishnan AN, Siegel CA, Sauer BG, Long MD. ACG Clinical Guideline: Ulcerative Colitis in Adults. Am J Gastroenterol. 2019;114(3):384-413.
35. Mostad I, Hovde O, Solberg IC, Moum BA. Clinical course and prognosis in ulcerative colitis: results from population-based and observational studies. Annals of Gastroenterology. 2014;27(2):10.
36. Lamb CA, Kennedy NA, Raine T, Hendy PA, Smith PJ, Limdi JK, et al. British Society of Gastroenterology consensus guidelines on the management of inflammatory bowel disease in adults. Gut. 2019;68(Suppl 3):s1-s106.
37. Fischer M, Siva S, Wo JM, Fadda HM. Assessment of Small Intestinal Transit Times in Ulcerative Colitis and Crohn's Disease Patients with Different Disease Activity Using Video Capsule Endoscopy. AAPS PharmSciTech. 2017;18(2):404-9.

38. Ho PM, Bryson CL, Rumsfeld JS. Medication adherence: its importance in cardiovascular outcomes. Circulation. 2009;119(23):3028-35.
39. D'Inca R, Bertomoro P, Mazzocco K, Vettorato MG, Rumiati R, Sturniolo GC. Risk factors for non-adherence to medication in inflammatory bowel disease patients. Aliment Pharmacol Ther. 2008;27(2):166-72.
40. Kane S, Hou D, Magnanti K. A pilot feasibility study of once daily versus conventional dosing mesalamine for maintenance of ulcerative colitis. Clinical gastroenterology and hepatology : the official clinical practice journal of the American Gastroenterological Association. 2003;1(3):170-3.
41. Quezada SM, McLean LP, Cross RK. Adverse events in IBD therapy: the 2018 update. Expert Rev Gastroenterol Hepatol. 2018;12(12):1183-91.
42. Rogler G. Gastrointestinal and liver adverse effects of drugs used for treating IBD. Best Pract Res Clin Gastroenterol. 2010;24(2):157-65.
43. Walsh LJ, Wong CA, Oborne J, Cooper S, Lewis SA, Pringle M, et al. Adverse effects of oral corticosteroids in relation to dose in patients with lung disease. Thorax. 2001;56(4):6.
44. Cunliffe RN, Scott BB. monitoring for drug side-effects in inflammatory bowel disease. Alimentary pharmacology & therapeutics. 2002;16(4):35.
45. Prantera C, Viscido A, Biancone L, Francavilla A, GiGlio L, Compieri M. A new oral delivery system for 5-ASA Preliminary clinical findings for MMx. Inflammatory bowel diseases. 2005;11(5):7.
46. Tønnesen HH, Karlsen J. Studies on curcumin and curcuminoids. VI. Kinetics of curcumin degradation in aqueous solution. Zeitschrift fur Lebensmittel-Untersuchung und -Forschung. 1985;180(5):3.
47. Zheng B, McClements DJ. Formulation of More Efficacious Curcumin Delivery Systems Using Colloid Science: Enhanced Solubility, Stability, and Bioavailability. Molecules. 2020;25(12).
48. Nelson KM, Dahlin JL, Bisson J, Graham J, Pauli GF, Walters MA. The Essential Medicinal Chemistry of Curcumin. J Med Chem. 2017;60(5):1620-37.
49. Jankun J, Wyganowska-Swiatkowska M, Dettlaff K, Jelinska A, Surdacka A, Watrobska-Swietlikowska D, et al. Determining whether curcumin degradation/condensation is actually bioactivation (Review). Int J Mol Med. 2016;37(5):1151-8.
50. Kumavat SD, Chaudhari Y, Borole P, Mishra PA. Degradation studies of curcumin. International Journal of Pharmacy Review & Research. 2013;3(2):6.
51. Zhu J, Sanidad KZ, Sukamtoh E, Zhang G. Potential roles of chemical degradation in the biological activities of curcumin. Food Funct. 2017;8(3):907-14.
52. Wang YJ, Pan MH, Cheng AL, Lin LI, Ho YS, Hsieh CY, et al. Stability of curcumin in buffer solutions and characterization of its degradation products. Stability of curcumin in buffer solutions and characterization of its degradation products Journal of pharmaceutical and biomedical analysis. 1997;15(12):10.
53. Treesinchai S, Pitaksuteepong T, Sungthongjeen S. Determination of curcumin stability in various gastrointestinal pH by Arrhenius equation using HPLC method. Pharmaceutical Sciences Asia. 2020;47(1):86-96.
54. Shen L, Ji HF. Theoretical study on physicochemical properties of curcumin. Spectrochim Acta A Mol Biomol Spectrosc. 2007;67(3-4):619-23.

55. Anand P, Kunnumakkara AB, Newman RA, Aggarwal BB. Bioavailability of curcumin: problems and promises. Mol Pharm. 2007;4(6):807-18.
56. Simadibrata M, Halimkesuma CC, Suwita BM. Efficacy of Curcumin as Adjuvant Therapy to Induce or Maintain Remission in Ulcerative Colitis Patients: an Evidence-based Clinical Review. Acta medica Indonesiana. 2017;49(4):6.
57. Borges A, Freitas V, Mateus N, Fernandes I, Oliveira J. Solid Lipid Nanoparticles as Carriers of Natural Phenolic Compounds. Antioxidants (Basel). 2020;9(10).
58. Shete H, Chatterjee S, De A, Patravale V. Long chain lipid based tamoxifen NLC. Part II: pharmacokinetic, biodistribution and in vitro anticancer efficacy studies. Int J Pharm. 2013;454(1):584-92.
59. Harde H, Das M, Jain S. Solid lipid nanoparticles: an oral bioavailability enhancer vehicle. Expert opinion on drug delivery. 2011;8(11):18.
60. Beloqui A, del Pozo-Rodríguez A, Isla A, Rodríguez-Gascón A, Solinís MÁ. Nanostructured lipid carriers as oral delivery systems for poorly soluble drugs. Journal of Drug Delivery Science and Technology. 2017;42:144-54.
61. Tamjidi F, Shahedi M, Varshosaz J, Nasirpour A. Nanostructured lipid carriers (NLC): A potential delivery system for bioactive food molecules. Innovative Food Science & Emerging Technologies. 2013;19:29-43.
62. Gaba B, Fazil M, Ali A, Baboota S, Sahni JK, Ali J. Nanostructured lipid (NLCs) carriers as a bioavailability enhancement tool for oral administration. Drug Deliv. 2015;22(6):691-700.
63. Tran TH, Ramasamy T, Truong DH, Choi HG, Yong CS, Kim JO. Preparation and characterization of fenofibrate-loaded nanostructured lipid carriers for oral bioavailability enhancement. AAPS PharmSciTech. 2014;15(6):1509-15.
64. Zhang N, Ping Q, Huang G, Xu W, Cheng Y, Han X. Lectin-modified solid lipid nanoparticles as carriers for oral administration of insulin. Int J Pharm. 2006;327(1-2):153-9.
65. Hua S, Marks E, Schneider JJ, Keely S. Advances in oral nano-delivery systems for colon targeted drug delivery in inflammatory bowel disease: selective targeting to diseased versus healthy tissue. Nanomedicine. 2015;11(5):1117-32.
66. Amidon S, Brown JE, Dave VS. Colon-targeted oral drug delivery systems: design trends and approaches. AAPS PharmSciTech. 2015;16(4):731-41.
67. Naeem M, Bae J, Oshi MA, Kim MS, Moon HR, Lee BL, et al. Colon-targeted delivery of cyclosporine A using dual-functional Eudragit((R)) FS30D/PLGA nanoparticles ameliorates murine experimental colitis. Int J Nanomedicine. 2018;13:1225-40.
68. Philip AK, Philip B. Colon targeted drug delivery systems: a review on primary and novel approaches. Oman Med J. 2010;25(2):79-87.
69. Shah NK, Rane BR, Gujarathi NA. Developments in colon specific drug delivery system - A review. Pharma Science Monitor. 2014;5(2):16.
70. Singh A, Sharma A, Kaur S. Micro carriers as colon drug delivery system: a review. International Journal of Research and Development in Pharmacy and Life Sciences. 2014;3(6):6.
71. Fukui E, Miyamura N, Uemura K, Kobayashi M. Preparation of enteric coated timed-release press-coated tablets and evaluation of their function by in vitro and in vivo tests for colon targeting. International Journal of Pharmaceutics. 2000;204:9.

72. Tiwari G, Tiwari R, Wal P, Wal A, Rai AK. Primary and novel approaches for colon targeted drug delivery – A review. International Journal of Drug Delivery. 2010;2(1):1-11.
73. Kothawade PD, Gangurde HH, Surawase RK, Wagh MA, Tamizharasi S. Conventional and novel approaches for colon specific drug delivery: A review. e-Journal of Science & Technology. 2011;6(2):25.
74. Chourasia MK, Jain SK. Pharmaceutical approaches to colon targeted drug delivery systems. Journal of Pharmacy & Pharmaceutical Sciences. 2003;6(1):34.
75. Maurer JM, Schellekens RC, van Rieke HM, Wanke C, Iordanov V, Stellaard F, et al. Gastrointestinal pH and Transit Time Profiling in Healthy Volunteers Using the IntelliCap System Confirms Ileo-Colonic Release of ColoPulse Tablets. PLoS One. 2015;10(7):e0129076.
76. Joshi M. Role of Eudragit in targeted drug delivery. International Journal of Current Pharmaceutical Research. 2013;5(2):5.
77. Barbosa JAC, Abdelsadig MSE, Conway BR, Merchant HA. Using zeta potential to study the ionisation behaviour of polymers employed in modified-release dosage forms and estimating their pKa. Int J Pharm X. 2019;1:100024.
78. Nayak UY, Mutalik S, Nayak Y. Polymethacrylate coated valsartan tablets for Ileo-colonic delivery formulation development and in vitro and in vivo evaluations. Research Journal of Pharmacy and Technology. 2013;6(12):8.
79. Nguyen DA, Fogler HS. Facilitated diffusion in the dissolution of carboxylic polymers. AIChE Journal. 2005;51(2):415-25.
80. Peppas NA, Narasimhan B. Mathematical models in drug delivery: how modeling has shaped the way we design new drug delivery systems. J Control Release. 2014;190:75-81.
81. Mathematical models of drug release. In: Bruschi ML, editor. Strategies to Modify the Drug Release from Pharmaceutical Systems: Woodhead Publishing; 2015. p. 63-86.
82. Modification of drug release. Strategies to Modify the Drug Release from Pharmaceutical Systems2015. p. 15-28.
83. Paarakh MP, Jose PA, CM S, Christoper GV. Release kinetics-concepts and applications. International Journal of Pharmacy Research & Technology. 2018;8:12-20.
84. Costa P, Lobo JMS. Modeling and comparison of dissolution profiles. European Journal of Pharmaceutical Sciences. 2001;13:123-33.
85. Paul DR. Elaborations on the Higuchi model for drug delivery. Int J Pharm. 2011;418(1):13-7.
86. Peppas NA, Sahlin JJ. A simple equation for the description of solute release, III Coupling of diffusion and relaxation. International Journal of Pharmaceutics. 1989;57:169-72.
87. Ritger PL, Peppas NA. A simple Equation for description of solute release

I. Fickian and non-Fickain release from non-swellable devices in the form of slabs, spheres, cylinders or discs. Journal of Controlled Release. 1987;5:23-36.
88. Hopfenberg HB. Controlled Release from Erodible Slabs, Cylinders, and Spheres. Controlled Release Polymeric Formulations. ACS Symposium Series1976. p. 26-32.

89. Chanburee S, Tiyaboonchai W. Mucoadhesive nanostructured lipid carriers (NLCs) as potential carriers for improving oral delivery of curcumin. Drug Dev Ind Pharm. 2017;43(3):432-40.
90. Marques MRC, Loebenberg R, Almukainzi M. Simulated Biological Fluids with Possible Application in Dissolution Testing. Dissolution Technologies. 2011;18(3):15-28.
91. Chowdhury AH, Lobo DN. Fluids and gastrointestinal function. Curr Opin Clin Nutr Metab Care. 2011;14(5):469-76.
92. Zhang Y, Huo M, Zhou J, Zou A, Li W, Yao C, et al. DDSolver: an add-in program for modeling and comparison of drug dissolution profiles. AAPS J. 2010;12(3):263-71.
93. Unagolla JM, Jayasuriya AC. Drug transport mechanisms and in vitro release kinetics of vancomycin encapsulated chitosan-alginate polyelectrolyte microparticles as a controlled drug delivery system. Eur J Pharm Sci. 2018;114:199-209.
94. Saha AK, ray S. Effect of cross linked biodegradable polymers on sustained release of sodium diclofenac loaded microspheres. Brazilian Journal of Pharmaceutical Sciences. 2013;49(4):16.
95. Tuyen Dao TP, Nguyen TH, To VV, Ho TH, Nguyen TA, Dang MC. A new formulation of curcumin using poly (lactic-co-glycolic acid)—polyethylene glycol diblock copolymer as carrier material. Advances in Natural Sciences: Nanoscience and Nanotechnology. 2014;5(3).
96. Hao S, Wang B, Wang Y. Porous hydrophilic core/hydrophobic shell nanoparticles for particle size and drug release control. Mater Sci Eng C Mater Biol Appl. 2015;49:51-7.
97. Kawashima Y, Niwa T, Takeuchi H, Hino T, Ito Y. Control of prolonged drug release and compression properties of ibuprofen microsponges with acrylic polymer , Eudragit RS, Changing their intraparticle porsosity. Chemical & pharmaceutical bulletin. 1992;40(1):6.
98. Bhise SB, More AB, Malayandi R. Formulation and in vitro evaluation of rifampicin loaded porous microspheres. Sci Pharm. 2010;78(2):291-302.
99. Fu Y, Kao WJ. Drug release kinetics and transport mechanisms of non-degradable and degradable polymeric delivery systems. Expert Opin Drug Deliv. 2010;7(4):429-44.
100. Hopfenberg HB, Stannett VT, Jacques CHM. The transport of methyl methacrylate monomer in Poly(methyl methacrylate). Journal of Applied Polymer Science. 1975;19:7.
101. Okunlola A, Adebayo AS, Adeyeye MC. Development of repaglinide microshpere using novel acetylated starches of bitter and Chinese yams as polymers. International Journal of Biological Macromolecules. 2017;94:10.
102. Nguyen C, Christensen JM, Nguyen T. Application of D-Optimal Study Design with Contour Surface Response for Designing Sustained Release Gliclazide Matrix Tablets. Pharmacology & Pharmacy. 2014;5:16.
103. Shah KU, Khan GM. Regulating drug release behavior and kinetics from matrix tablets based on fine particle-sized ethyl cellulose ether derivatives: an in vitro and in vivo evaluation. ScientificWorldJournal. 2012;2012:842348.
104. Zhao YN, Xu X, Wen N, Song R, Meng Q, Guan Y, et al. A Drug Carrier for Sustained Zero-Order Release of Peptide Therapeutics. Sci Rep. 2017;7(1):5524.

105. Lanoizele E, Deratani A, Menut P, line P-B, Dupuy C. Elaboration of porous poly(ether-imide) membrane using vapor induced phase separation. Songklanakarin Journal of Science and Technology. 2002;24:7.
106. Beloqui A, Coco R, Memvanga PB, Ucakar B, des Rieux A, Preat V. pH-sensitive nanoparticles for colonic delivery of curcumin in inflammatory bowel disease. Int J Pharm. 2014;473(1-2):203-12.
107. Jubeh TT, Barenholz Y, Rubinstein A. Differential adhesion of normal and inflamed rat colonic mucosa by charged liposomes. Pharmaceutical Research. 2004;21(3):7.
108. Tirosh B, Khatib N, Barenholz Y, Nissan A, Rubinstein A. Transferrin as a luminal target for negatively charged liposomes in the inflamed colonic mucosa. Moleular Pharmaceutics. 2008;6(4):9.
109. Schneider C, Gordon ON, Edwards RL, Luis PB. Degradation of Curcumin: From Mechanism to Biological Implications. J Agric Food Chem. 2015;63(35):7606-14.

# APPENDIX

**Table 12 Percentage of drug loading of curcumin-NLCs lyophilized powder**

| No. | Weight (mg) | Peak area | concentrations (µg/ml) | amount of Curcumin (µg) in NLC-powder 1 mg | avg | %Drug loading | mean | SD |
|---|---|---|---|---|---|---|---|---|
| 1.1 | 10.2 | 155664 | 1.4836 | 2.9090 | 2.7451 | 0.2745 | 0.2843 | 0.0211 |
| 1.1 | 10.2 | 155845 | 1.4853 | 2.9123 | | | | |
| 1.2 | 10.9 | 147683 | 1.4084 | 2.5842 | | | | |
| 1.2 | 10.9 | 147140 | 1.4033 | 2.5749 | | | | |
| 2.1 | 10.5 | 145703 | 1.3898 | 2.6472 | 2.64798 | 0.2648 | | |
| 2.1 | 10.5 | 145869 | 1.3913 | 2.6501 | | | | |
| 2.2 | 10.7 | 145138 | 1.3844 | 2.5877 | | | | |
| 2.2 | 10.7 | 151905 | 1.4482 | 2.7069 | | | | |
| 3.1 | 11.8 | 188703 | 1.7948 | 3.0420 | 3.13527 | 0.3135 | | |
| 3.1 | 11.8 | 196698 | 1.8701 | 3.1696 | | | | |
| 3.2 | 9.2 | 157253 | 1.4985 | 3.2577 | | | | |
| 3.2 | 9.2 | 148171 | 1.4130 | 3.0718 | | | | |

**Table 13 Percentage of drug loading of curcumin-NLC 7ES beads**

| No. | Weight (mg) | Peak area | concentrations (µg/ml) | amount of Curcumin (µg) in NLC-beads 1 mg | avg | %Drug loading | mean | SD |
|---|---|---|---|---|---|---|---|---|
| 1.1 | 21 | 104555 | 1.0022 | 1.9089 | 1.6628 | 0.1663 | 0.1444 | 0.0158 |
| 1.1 | 21 | 88297 | 0.8491 | 1.6172 | | | | |
| 1.2 | 20.9 | 84025 | 0.8088 | 1.5480 | | | | |
| 1.2 | 20.9 | 85646 | 0.8241 | 1.5772 | | | | |
| 2.1 | 21.4 | 70943 | 0.6856 | 1.2815 | 1.2974 | 0.1297 | | |
| 2.1 | 21.4 | 72289 | 0.6983 | 1.3052 | | | | |
| 2.2 | 20.1 | 64795 | 0.6277 | 1.2491 | | | | |
| 2.2 | 20.1 | 70383 | 0.6803 | 1.3539 | | | | |
| 3.1 | 21 | 82680 | 0.7961 | 1.5165 | 1.3719 | 0.1372 | | |
| 3.1 | 21 | 69360 | 0.6707 | 1.2775 | | | | |
| 3.2 | 21.7 | 70898 | 0.6852 | 1.2630 | | | | |
| 3.2 | 21.7 | 80559 | 0.7762 | 1.4307 | | | | |

**Table 14 Percentage of drug loading of curcumin-NLC 9ES beads**

| No. | Weight (mg) | Peak area | concentrations (µg/ml) | amount of Curcumin (µg) in NLC-beads 1 mg | avg | %Drug loading | mean | SD |
|---|---|---|---|---|---|---|---|---|
| 1.1 | 21.5 | 55004 | 0.5355 | 0.9962 | 0.9164 | 0.0916 | 0.0977 | 0.0046 |
| 1.1 | 21.5 | 53312 | 0.5195 | 0.9666 | | | | |
| 1.2 | 23.4 | 50606 | 0.4940 | 0.8445 | | | | |
| 1.2 | 23.4 | 51458 | 0.5021 | 0.8582 | | | | |
| 2.1 | 21.8 | 57266 | 0.5568 | 1.0216 | 1.0272 | 0.1027 | | |
| 2.1 | 21.8 | 57209 | 0.5562 | 1.0206 | | | | |
| 2.2 | 22.3 | 58541 | 0.5688 | 1.0202 | | | | |
| 2.2 | 22.3 | 60081 | 0.5833 | 1.0462 | | | | |
| 3.1 | 22.7 | 60916 | 0.5911 | 1.0417 | 0.9860 | 0.0986 | | |
| 3.1 | 22.7 | 62279 | 0.6040 | 1.0643 | | | | |
| 3.2 | 24.3 | 57625 | 0.5601 | 0.9221 | | | | |
| 3.2 | 24.3 | 57241 | 0.5565 | 0.9161 | | | | |

**Table 15 Percentage of drug entrapment efficiency of curcumin-NLCs lyophilized powder**

| No. | Peak area | Conc. (µg/ml) | amount of Curcumin (mg) in NLC-powders | %Drug entrapment | SD |
|---|---|---|---|---|---|
| 1.1 | 183858 | 1.7491 | 90.96 | | |
| 1.2 | 184800 | 1.7580 | 91.42 | | |
| 2.1 | 168590 | 1.6053 | 83.48 | 90.78 | 6.22 |
| 2.2 | 166755 | 1.5880 | 82.58 | | |
| 3.1 | 199801 | 1.8993 | 96.86 | | |
| 3.2 | 205075 | 1.9490 | 99.40 | | |

**Table 16 Percentage of drug entrapment efficiency of curcumin-NLC 7ES beads**

| | Peak area | Conc. (µg/ml) | amount of Curcumin (mg) in NLC-beads | %Drug entrapment | SD |
|---|---|---|---|---|---|
| 1.1 | 190703 | 1.8136 | 83.96 | | |
| 1.2 | 184330 | 1.7536 | 81.18 | | |
| 2.1 | 200822 | 1.9089 | 88.38 | 82.08 | 4.91 |
| 2.2 | 169854 | 1.6172 | 74.87 | | |
| 3.1 | 174951 | 1.6652 | 77.09 | | |
| 3.2 | 197621 | 1.8788 | 86.98 | | |

**Table 17 Percentage of drug entrapment efficiency of curcumin-NLC 9ES beads**

| No. | Peak area | Conc. (µg/ml) | amount of Curcumin (mg) in NLC-beads | %Drug entrapment | SD |
|---|---|---|---|---|---|
| 1.1 | 126943 | 1.2131 | 101.09 | | |
| 1.2 | 129113 | 1.2335 | 102.79 | | |
| 2.1 | 112315 | 1.0753 | 89.61 | 93.68 | 6.02 |
| 2.2 | 111056 | 1.0634 | 88.62 | | |
| 3.1 | 115636 | 1.1066 | 92.21 | | |
| 3.2 | 109947 | 1.0530 | 87.75 | | |

**Table 18 Cumulative percentage released of curcumin-NLC 7ES bead in simulated GI tract condition medium (FaSSGF ;pH 1.6 ,and FaSSIF ;pH 6.5-7.4)**

| Time (h) | No. | Peak area | Conc. in 100 ml | Cumulative amount (µg) | Cumulative release (%) | Mean | SD |
|---|---|---|---|---|---|---|---|
| 1 | 1 | ND | ND | ND | ND | | |
| | 2 | ND | ND | ND | ND | ND | ND |
| | 3 | ND | ND | ND | ND | | |
| 2 | 1 | ND | ND | ND | ND | | |
| | 2 | ND | ND | ND | ND | ND | ND |
| | 3 | ND | ND | ND | ND | | |
| 2.5 | 1 | ND | ND | ND | ND | | |
| | 2 | ND | ND | ND | ND | ND | ND |
| | 3 | ND | ND | ND | ND | | |
| 3 | 1 | 1804 | 11.97 | 12.63 | 7.65 | | |
| | 2 | 1885 | 12.13 | 12.80 | 7.79 | 7.77 | 0.11 |
| | 3 | 1913 | 12.18 | 12.86 | 7.86 | | |
| 4 | 1 | 7281 | 22.86 | 25.92 | 15.71 | | |
| | 2 | 7417 | 23.13 | 26.23 | 15.97 | 16.00 | 1.51 |
| | 3 | 7615 | 23.52 | 26.67 | 16.31 | | |
| 5 | 1 | 14281 | 36.78 | 45.03 | 27.29 | | |
| | 2 | 14429 | 37.07 | 45.39 | 27.64 | 27.67 | 0.77 |
| | 3 | 14641 | 37.50 | 45.91 | 28.08 | | |
| 5.5 | 1 | 16697 | 41.58 | 53.16 | 32.22 | | |
| | 2 | 17092 | 42.37 | 54.16 | 32.99 | 33.10 | 1.19 |
| | 3 | 17719 | 43.62 | 55.75 | 34.10 | | |
| 6 | 1 | 29463 | 66.97 | 89.19 | 54.05 | | |
| | 2 | 30422 | 68.88 | 91.72 | 55.86 | 54.36 | 1.64 |
| | 3 | 28586 | 65.23 | 86.91 | 53.16 | | |
| 7 | 1 | 33126 | 74.26 | 108.33 | 65.65 | | |
| | 2 | 34278 | 76.55 | 111.66 | 68.00 | 67.92 | 3.11 |
| | 3 | 35313 | 78.61 | 114.62 | 70.10 | | |
| 9 | 1 | 28316 | 64.69 | 116.37 | 70.52 | | |
| | 2 | 27266 | 62.60 | 112.74 | 68.66 | 69.98 | 1.70 |
| | 3 | 28112 | 64.29 | 115.71 | 70.77 | | |
| 12 | 1 | 22580 | 53.28 | 145.79 | 88.35 | | |
| | 2 | 22117 | 52.36 | 143.39 | 86.90 | 87.73 | 5.23 |
| | 3 | 22443 | 53.01 | 145.15 | 87.96 | | |

*ND = No detected

**Table 19 Cumulative percentage released of curcumin-NLC 9ES bead in simulated GI tract condition medium (FaSSGF ;pH 1.6 ,and FaSSIF ;pH 6.5-7.4)**

| Time (h) | No. | Peak area | Conc. in 100 ml | Cumulative amount (µg) | Cumulative release (%) | Mean | SD |
|---|---|---|---|---|---|---|---|
| 1 | 1 | ND | ND | ND | ND | | |
| | 2 | ND | ND | ND | ND | ND | ND |
| | 3 | ND | ND | ND | ND | | |
| 2 | 1 | ND | ND | ND | ND | | |
| | 2 | ND | ND | ND | ND | ND | ND |
| | 3 | ND | ND | ND | ND | | |
| 2.5 | 1 | ND | ND | ND | ND | | |
| | 2 | ND | ND | ND | ND | ND | ND |
| | 3 | ND | ND | ND | ND | | |
| 3 | 1 | ND | ND | ND | ND | | |
| | 2 | ND | ND | ND | ND | ND | ND |
| | 3 | ND | ND | ND | ND | | |
| 4 | 1 | 3138 | 14.62 | 16.54 | 13.65 | | |
| | 2 | 3347 | 15.04 | 17.01 | 14.09 | 14.21 | 0.53 |
| | 3 | 3760 | 15.86 | 17.94 | 14.88 | | |
| 5 | 1 | 5092 | 18.50 | 22.64 | 18.69 | | |
| | 2 | 4970 | 18.26 | 22.35 | 18.51 | 18.66 | 0.64 |
| | 3 | 5080 | 18.48 | 22.62 | 18.77 | | |
| 5.5 | 1 | 10582 | 29.42 | 37.50 | 30.97 | | |
| | 2 | 10574 | 29.41 | 37.48 | 31.06 | 30.95 | 0.29 |
| | 3 | 10430 | 29.12 | 37.13 | 30.81 | | |
| 6 | 1 | 13960 | 36.14 | 48.14 | 39.76 | | |
| | 2 | 13826 | 35.88 | 47.79 | 39.60 | 40.22 | 1.95 |
| | 3 | 14575 | 37.36 | 49.76 | 41.30 | | |
| 7 | 1 | 16484 | 41.16 | 60.04 | 49.58 | | |
| | 2 | 16478 | 41.15 | 60.03 | 49.73 | 50.19 | 0.97 |
| | 3 | 17084 | 42.35 | 61.78 | 51.27 | | |
| 9 | 1 | 16796 | 41.78 | 74.95 | 61.89 | | |
| | 2 | 17080 | 42.35 | 75.94 | 62.92 | 63.14 | 1.72 |
| | 3 | 17614 | 43.41 | 77.85 | 64.60 | | |
| 12 | 1 | 18555 | 45.28 | 122.70 | 101.32 | | |
| | 2 | 18314 | 44.80 | 121.44 | 100.61 | 98.86 | 3.87 |
| | 3 | 16902 | 41.99 | 114.04 | 94.64 | | |

*ND = No detected

**Table 20 Cumulative percentage released of curcumin-NLCs in simulated GI tract condition medium (FaSSGF;pH 1.6)**

| Time (h) | No. | Peak area | Conc. in 100 ml | Cumulative amount (µg) | Cumulative release (%) | Mean | SD |
|---|---|---|---|---|---|---|---|
| 0.5 | 1 | 4997 | 18.32 | 18.32 | 27.88 | | |
| | 2 | 5827 | 19.97 | 19.97 | 24.34 | 24.13 | 3.17 |
| | 3 | 4183 | 16.70 | 16.70 | 20.17 | | |
| 1 | 1 | 16576 | 41.34 | 41.44 | 63.09 | | |
| | 2 | 16182 | 40.56 | 40.66 | 49.56 | 54.49 | 6.12 |
| | 3 | 16894 | 41.98 | 42.06 | 50.81 | | |
| 2 | 1 | 17109 | 42.40 | 42.71 | 65.01 | | |
| | 2 | 18860 | 45.89 | 46.19 | 56.30 | 60.18 | 3.62 |
| | 3 | 20295 | 48.74 | 49.03 | 59.24 | | |
| 3 | 1 | 16652 | 41.50 | 42.02 | 63.95 | | |
| | 2 | 17627 | 43.43 | 43.97 | 53.59 | 57.27 | 5.32 |
| | 3 | 18101 | 44.38 | 44.91 | 54.26 | | |

**Table 21 Cumulative percentage released of curcumin-NLCs in simulated GI tract condition medium (FaSSIF ;pH 6.5-7.4)**

| Time (h) | No. | Peak area | Conc. in 100 ml | Cumulative amount (µg) | Cumulative release (%) | Mean | SD |
|---|---|---|---|---|---|---|---|
| 0.5 | 1 | 16043 | 40.28 | 41.87 | 63.73 | | |
| | 2 | 17083 | 42.35 | 44.01 | 53.64 | 53.50 | 8.41 |
| | 3 | 12981 | 34.19 | 35.69 | 43.12 | | |
| 1 | 1 | 17610 | 43.40 | 46.77 | 71.19 | | |
| | 2 | 17666 | 43.51 | 46.93 | 57.20 | 60.67 | 7.59 |
| | 3 | 16464 | 41.12 | 44.37 | 53.61 | | |
| 2 | 1 | 19008 | 46.18 | 53.52 | 81.46 | | |
| | 2 | 20784 | 49.71 | 57.56 | 70.16 | 71.19 | 8.20 |
| | 3 | 18012 | 44.20 | 51.27 | 61.94 | | |
| 3 | 1 | 19720 | 47.60 | 59.66 | 90.81 | | |
| | 2 | 21299 | 50.74 | 63.56 | 77.47 | 79.44 | 8.95 |
| | 3 | 19032 | 46.23 | 57.98 | 70.05 | | |
| 3.5 | 1 | 18454 | 45.08 | 59.17 | 90.07 | | |
| | 2 | 21358 | 50.85 | 66.59 | 81.16 | 81.16 | 7.28 |
| | 3 | 18712 | 45.59 | 59.80 | 72.24 | | |
| 4 | 1 | 17993 | 44.16 | 60.74 | 92.45 | | |
| | 2 | 18944 | 46.05 | 63.37 | 77.25 | 82.56 | 7.21 |
| | 3 | 19454 | 47.07 | 64.56 | 77.99 | | |
| 5 | 1 | 15033 | 38.28 | 58.13 | 88.48 | | |
| | 2 | 17835 | 43.85 | 66.32 | 80.84 | 81.25 | 5.77 |
| | 3 | 16248 | 40.69 | 61.61 | 74.43 | | |
| 7 | 1 | 10684 | 29.63 | 56.22 | 85.58 | | |
| | 2 | 13021 | 34.27 | 64.67 | 78.83 | 81.09 | 3.18 |
| | 3 | 13254 | 34.74 | 65.26 | 78.84 | | |
| 9 | 1 | 6024 | 20.36 | 44.92 | 68.38 | | |
| | 2 | 7492 | 23.28 | 51.02 | 62.18 | 64.69 | 2.71 |
| | 3 | 7949 | 24.19 | 52.56 | 63.49 | | |

**Table 22 Stability of curcumin-NLC lyophilized powder at room temperature after 1 month**

| NLCs | Weight (mg) | Peak area | Concentrations (µg /ml) | amount of Curcumin in 1 mg | avg | %Drug remaining | mean | SD |
|---|---|---|---|---|---|---|---|---|
| 1.1 | 10.1 | 143951 | 1.3733 | 2.7193 | 2.5665 | 92.30 | | |
| 1.1 | 10.1 | 143889 | 1.3727 | 2.7182 | | | | |
| 1.2 | 9.8 | 123272 | 1.1785 | 2.4051 | | | | |
| 1.2 | 9.8 | 124221 | 1.1874 | 2.4233 | | | | |
| 2.1 | 10.4 | 140912 | 1.3446 | 2.5858 | 2.5606 | 97.33 | | |
| 2.1 | 10.4 | 143847 | 1.3723 | 2.6390 | | | 91.05 | 5.71 |
| 2.2 | 11.5 | 151048 | 1.4401 | 2.5045 | | | | |
| 2.2 | 11.5 | 151570 | 1.4450 | 2.5131 | | | | |
| 3.1 | 10.8 | 151844 | 1.4476 | 2.6807 | 2.6384 | 83.51 | | |
| 3.1 | 10.8 | 154935 | 1.4767 | 2.7347 | | | | |
| 3.2 | 9.6 | 129111 | 1.2335 | 2.5697 | | | | |
| 3.2 | 9.6 | 129038 | 1.2328 | 2.5683 | | | | |

**Table 23 Stability of curcumin-NLC lyophilized powder at 4 degrees Celsius after 1 month**

| NLCs | Weight (mg) | Peak area | Concentrations (µg /ml) | amount of Curcumin in 1 mg | avg | %Drug remaining | mean | SD |
|---|---|---|---|---|---|---|---|---|
| 1.1 | 11.4 | 174952 | 1.6653 | 2.9215 | 2.7526 | 100.27 | | |
| 1.1 | 11.4 | 176882 | 1.6834 | 2.9534 | | | | |
| 1.2 | 10.6 | 143774 | 1.3716 | 2.5879 | | | | |
| 1.2 | 10.6 | 141512 | 1.3503 | 2.5477 | | | | |
| 2.1 | 10.6 | 145542 | 1.3882 | 2.6193 | 2.6018 | 98.25 | | |
| 2.1 | 10.6 | 146665 | 1.3988 | 2.6393 | | | 97.25 | 2.96 |
| 2.2 | 9.9 | 133181 | 1.2718 | 2.5693 | | | | |
| 2.2 | 9.9 | 133696 | 1.2767 | 2.5791 | | | | |
| 3.1 | 9.9 | 151959 | 1.4487 | 2.9266 | 2.9232 | 93.23 | | |
| 3.1 | 9.9 | 155667 | 1.4836 | 2.9972 | | | | |
| 3.2 | 10.1 | 152293 | 1.4518 | 2.8749 | | | | |
| 3.2 | 10.1 | 153313 | 1.4614 | 2.8939 | | | | |

**Table 24 Stability of curcumin-NLC lyophilized powder at room temperature after 3 months**

| NLCs | Weight (mg) | Peak area | Concentrations (µg /ml) | amount of Curcumin in 1 mg | avg | %Drug remaining | mean | SD |
|---|---|---|---|---|---|---|---|---|
| 1.1 | 10.4 | 130538 | 1.2469 | 2.3979 | 2.4338 | 87.53 | 90.03 | 1.85 |
| 1.1 | 10.4 | 135584 | 1.2944 | 2.4893 | | | | |
| 1.2 | 9.4 | 120538 | 1.1527 | 2.4526 | | | | |
| 1.2 | 9.4 | 117684 | 1.1258 | 2.3954 | | | | |
| 2.1 | 10.4 | 136061 | 1.2989 | 2.4980 | 2.4193 | 91.96 | | |
| 2.1 | 10.4 | 141007 | 1.3455 | 2.5876 | | | | |
| 2.2 | 9.8 | 118327 | 1.1319 | 2.3100 | | | | |
| 2.2 | 9.8 | 116852 | 1.1180 | 2.2817 | | | | |
| 3.1 | 10.7 | 158039 | 1.5060 | 2.8149 | 2.8624 | 90.61 | | |
| 3.1 | 10.7 | 157019 | 1.4963 | 2.7969 | | | | |
| 3.2 | 10.4 | 158717 | 1.5123 | 2.9083 | | | | |
| 3.2 | 10.4 | 159890 | 1.5234 | 2.9296 | | | | |

**Table 25 Stability of curcumin-NLC lyophilized powder at 4 degrees Celsius after 3 months**

| NLCs | Weight (mg) | Peak area | Concentrations (µg /ml) | amount of Curcumin in 1 mg | avg | %Drug remaining | mean | SD |
|---|---|---|---|---|---|---|---|---|
| 1.1 | 11.8 | 178063 | 1.6946 | 2.8721 | 2.7391 | 99.78 | 92.02 | 9.56 |
| 1.1 | 11.8 | 178489 | 1.6986 | 2.8789 | | | | |
| 1.2 | 11.5 | 156981 | 1.4960 | 2.6017 | | | | |
| 1.2 | 11.5 | 157095 | 1.4971 | 2.6036 | | | | |
| 2.1 | 10 | 133466 | 1.2745 | 2.5490 | 2.5875 | 97.72 | | |
| 2.1 | 10 | 132586 | 1.2662 | 2.5324 | | | | |
| 2.2 | 9.3 | 127319 | 1.2166 | 2.6163 | | | | |
| 2.2 | 9.3 | 129096 | 1.2333 | 2.6523 | | | | |
| 3.1 | 9.6 | 110276 | 1.0561 | 2.2001 | 2.4630 | 78.56 | | |
| 3.1 | 9.6 | 108972 | 1.0438 | 2.1746 | | | | |
| 3.2 | 10.6 | 149655 | 1.4270 | 2.6924 | | | | |
| 3.2 | 10.6 | 154846 | 1.4759 | 2.7847 | | | | |

**Table 26 Stability of curcumin-NLC lyophilized powder at room temperature after 6 months**

| NLCs | Weight (mg) | Peak area | Concentrations (µg /ml) | amount of Curcumin in 1 mg | avg | %Drug remaining | mean | SD |
|---|---|---|---|---|---|---|---|---|
| 1.1 | 10.9 | 148522 | 1.4163 | 2.5987 | 2.4519 | 88.18 | 88.90 | 4.32 |
| 1.1 | 10.9 | 152903 | 1.4576 | 2.6745 | | | | |
| 1.2 | 11 | 129603 | 1.2381 | 2.2511 | | | | |
| 1.2 | 11 | 131488 | 1.2559 | 2.2834 | | | | |
| 2.1 | 9.9 | 128716 | 1.2298 | 2.4844 | 2.4867 | 94.52 | | |
| 2.1 | 9.9 | 129117 | 1.2335 | 2.4920 | | | | |
| 2.2 | 9.9 | 130150 | 1.2433 | 2.5116 | | | | |
| 2.2 | 9.9 | 127366 | 1.2170 | 2.4587 | | | | |
| 3.1 | 11.5 | 171126 | 1.6292 | 2.8334 | 2.6540 | 84.01 | | |
| 3.1 | 11.5 | 167712 | 1.5971 | 2.7775 | | | | |
| 3.2 | 10.6 | 140085 | 1.3368 | 2.5223 | | | | |
| 3.2 | 10.6 | 137865 | 1.3159 | 2.4829 | | | | |

**Table 27 Stability of curcumin-NLC lyophilized powder at 4 degrees Celsius after 6 months**

| NLCs | Weight (mg) | Peak area | Concentrations (µg /ml) | amount of Curcumin in 1 mg | avg | %Drug remaining | mean | SD |
|---|---|---|---|---|---|---|---|---|
| 1.1 | 9.3 | 123463 | 1.1803 | 2.5382 | 2.4403 | 88.90 | 91.09 | 1.86 |
| 1.1 | 9.3 | 123855 | 1.1840 | 2.5462 | | | | |
| 1.2 | 10.8 | 133560 | 1.2754 | 2.3618 | | | | |
| 1.2 | 10.8 | 130873 | 1.2501 | 2.3150 | | | | |
| 2.1 | 11.4 | 151392 | 1.4433 | 2.5322 | 2.4742 | 93.44 | | |
| 2.1 | 11.4 | 151345 | 1.4429 | 2.5314 | | | | |
| 2.2 | 10.7 | 132298 | 1.2635 | 2.3617 | | | | |
| 2.2 | 10.7 | 138538 | 1.3223 | 2.4715 | | | | |
| 3.1 | 10.4 | 159123 | 1.5162 | 2.9157 | 2.8514 | 90.95 | | |
| 3.1 | 10.4 | 153912 | 1.4671 | 2.8213 | | | | |
| 3.2 | 10.6 | 160174 | 1.5261 | 2.8794 | | | | |
| 3.2 | 10.6 | 155104 | 1.4783 | 2.7893 | | | | |

**Table 28 Stability of curcumin-NLC 7ES bead powder at room temperature after 1 month**

| 7ES | Weight (mg) | Peak area | Concentrations (µg /ml) | amount of Curcumin in 1 mg | avg | %Drug remaining | mean | SD |
|---|---|---|---|---|---|---|---|---|
| 1.1 | 21 | 61906 | 0.6005 | 1.1438 | 1.1895 | 71.85 | 60.79 | 8.05 |
| 1.1 | 21 | 68034 | 0.6582 | 1.2537 | | | | |
| 1.2 | 20.1 | 60820 | 0.5902 | 1.1746 | | | | |
| 1.2 | 20.1 | 61420 | 0.5959 | 1.1859 | | | | |
| 2.1 | 20.4 | 37500 | 0.3706 | 0.7267 | 0.7305 | 52.94 | | |
| 2.1 | 20.4 | 37887 | 0.3742 | 0.7338 | | | | |
| 2.2 | 22.6 | 42244 | 0.4153 | 0.7350 | | | | |
| 2.2 | 22.6 | 41744 | 0.4106 | 0.7267 | | | | |
| 3.1 | 21.1 | 35873 | 0.3553 | 0.6735 | 0.7427 | 57.56 | | |
| 3.1 | 21.1 | 41910 | 0.4121 | 0.7813 | | | | |
| 3.2 | 21.1 | 39917 | 0.3934 | 0.7457 | | | | |
| 3.2 | 21.1 | 41297 | 0.4064 | 0.7703 | | | | |

**Table 29 Stability of curcumin-NLC 7ES bead powder at 4 degrees Celsius after 1 month**

| 7ES | Weight (mg) | Peak area | Concentrations (µg /ml) | amount of Curcumin in 1 mg | avg | %Drug remaining | mean | SD |
|---|---|---|---|---|---|---|---|---|
| 1.1 | 21.9 | 88381 | 0.8498 | 1.5522 | 1.6555 | 99.56 | 96.20 | 6.89 |
| 1.1 | 21.9 | 86843 | 0.8354 | 1.5258 | | | | |
| 1.2 | 20.6 | 89205 | 0.8576 | 1.6652 | | | | |
| 1.2 | 20.6 | 100880 | 0.9676 | 1.8788 | | | | |
| 2.1 | 18 | 68072 | 0.6586 | 1.4634 | 1.3291 | 102.45 | | |
| 2.1 | 18 | 63254 | 0.6132 | 1.3626 | | | | |
| 2.2 | 22.8 | 68791 | 0.6653 | 1.1672 | | | | |
| 2.2 | 22.8 | 78234 | 0.7543 | 1.3233 | | | | |
| 3.1 | 23.4 | 65496 | 0.6343 | 1.0843 | 1.1882 | 86.61 | | |
| 3.1 | 23.4 | 73202 | 0.7069 | 1.2083 | | | | |
| 3.2 | 25 | 80233 | 0.7731 | 1.2370 | | | | |
| 3.2 | 25 | 79315 | 0.7644 | 1.2231 | | | | |

**Table 30 Stability of curcumin-NLC 7ES bead powder at room temperature after 3 months**

| 7ES | Weight (mg) | Peak area | Concentrations (µg /ml) | amount of Curcumin in 1 mg | avg | %Drug remaining | mean | SD |
|---|---|---|---|---|---|---|---|---|
| 1.1 | 20.5 | 46574 | 0.4561 | 0.8899 | 0.8019 | 48.44 | | |
| 1.1 | 20.5 | 45443 | 0.4454 | 0.8691 | | | | |
| 1.2 | 20.8 | 38605 | 0.3810 | 0.7327 | | | | |
| 1.2 | 20.8 | 37682 | 0.3723 | 0.7160 | | | | |
| 2.1 | 21.3 | 28243 | 0.2834 | 0.5322 | 0.4925 | 35.70 | | |
| 2.1 | 21.3 | 25421 | 0.2568 | 0.4823 | | | | |
| 2.2 | 20.9 | 24694 | 0.2500 | 0.4784 | | | 40.20 | 5.83 |
| 2.2 | 20.9 | 24630 | 0.2494 | 0.4773 | | | | |
| 3.1 | 20.4 | 22513 | 0.2294 | 0.4499 | 0.4706 | 36.47 | | |
| 3.1 | 20.4 | 25371 | 0.2563 | 0.5026 | | | | |
| 3.2 | 21 | 24071 | 0.2441 | 0.4650 | | | | |
| 3.2 | 21 | 24071 | 0.2441 | 0.4650 | | | | |

**Table 31 Stability of curcumin-NLC 7ES bead powder at 4 degrees Celsius after 3 months**

| 7ES | Weight (mg) | Peak area | Concentrations (µg /ml) | amount of Curcumin in 1 mg | avg | %Drug remaining | mean | SD |
|---|---|---|---|---|---|---|---|---|
| 1.1 | 21.8 | 91413 | 0.8784 | 1.6117 | 1.5819 | 95.13 | | |
| 1.1 | 21.8 | 91310 | 0.8774 | 1.6100 | | | | |
| 1.2 | 21.5 | 86884 | 0.8357 | 1.5549 | | | | |
| 1.2 | 21.5 | 86665 | 0.8337 | 1.5510 | | | | |
| 2.1 | 20.1 | 56184 | 0.5466 | 1.0877 | 1.1688 | 90.09 | | |
| 2.1 | 20.1 | 58308 | 0.5666 | 1.1275 | | | | |
| 2.2 | 20.8 | 67337 | 0.6516 | 1.2531 | | | 91.73 | 2.41 |
| 2.2 | 20.8 | 64787 | 0.6276 | 1.2069 | | | | |
| 3.1 | 21.8 | 61796 | 0.5994 | 1.0999 | 1.2342 | 89.96 | | |
| 3.1 | 21.8 | 61380 | 0.5955 | 1.0927 | | | | |
| 3.2 | 19.9 | 70471 | 0.6811 | 1.3691 | | | | |
| 3.2 | 19.9 | 70785 | 0.6841 | 1.3751 | | | | |

**Table 32 Stability of curcumin-NLC 7ES bead powder at room temperature after 6 months**

| 7ES | Weight (mg) | Peak area | Concentrations (µg /ml) | amount of Curcumin in 1 mg | avg | %Drug remaining | mean | SD |
|---|---|---|---|---|---|---|---|---|
| 1.1 | 20.6 | 37813 | 0.3735 | 0.7253 | 0.7092 | 42.84 | | |
| 1.1 | 20.6 | 33669 | 0.3345 | 0.6495 | | | | |
| 1.2 | 19.7 | 35136 | 0.3483 | 0.7073 | | | | |
| 1.2 | 19.7 | 37606 | 0.3716 | 0.7545 | | | | |
| 2.1 | 20.7 | 19093 | 0.1972 | 0.3811 | 0.3933 | 28.50 | | |
| 2.1 | 20.7 | 18674 | 0.1933 | 0.3735 | | | | |
| 2.2 | 21.1 | 21794 | 0.2227 | 0.4221 | | | 33.65 | 6.51 |
| 2.2 | 21.1 | 20358 | 0.2091 | 0.3965 | | | | |
| 3.1 | 21.3 | 20824 | 0.2135 | 0.4010 | 0.3819 | 29.60 | | |
| 3.1 | 21.3 | 22337 | 0.2278 | 0.4277 | | | | |
| 3.2 | 20.3 | 17225 | 0.1796 | 0.3539 | | | | |
| 3.2 | 20.3 | 16748 | 0.1751 | 0.3451 | | | | |

**Table 33 Stability of curcumin-NLC 7ES bead powder at 4 degrees Celsius after 6 months**

| 7ES | Weight (mg) | Peak area | Concentrations (µg /ml) | amount of Curcumin in 1 mg | avg | %Drug remaining | mean | SD |
|---|---|---|---|---|---|---|---|---|
| 1.1 | 21 | 76241 | 0.7355 | 1.4009 | 1.4597 | 87.78 | | |
| 1.1 | 21 | 80572 | 0.7763 | 1.4786 | | | | |
| 1.2 | 20.4 | 78225 | 0.7542 | 1.4788 | | | | |
| 1.2 | 20.4 | 78308 | 0.7550 | 1.4803 | | | | |
| 2.1 | 21 | 62484 | 0.6059 | 1.1541 | 1.1340 | 87.41 | | |
| 2.1 | 21 | 63098 | 0.6117 | 1.1651 | | | | |
| 2.2 | 20.3 | 58495 | 0.5683 | 1.1199 | | | 87.15 | 0.64 |
| 2.2 | 20.3 | 57259 | 0.5567 | 1.0970 | | | | |
| 3.1 | 20.4 | 61701 | 0.5985 | 1.1736 | 1.1836 | 86.28 | | |
| 3.1 | 20.4 | 59165 | 0.5747 | 1.1268 | | | | |
| 3.2 | 20.5 | 63717 | 0.6175 | 1.2049 | | | | |
| 3.2 | 20.5 | 65035 | 0.6299 | 1.2292 | | | | |

**Table 34 Stability of curcumin-NLC 9ES bead powder at room temperature after 1 month**

| 9ES | Weight (mg) | Peak area | Concentrations (µg /ml) | amount of Curcumin in 1 mg | avg | %Drug remaining | mean | SD |
|---|---|---|---|---|---|---|---|---|
| 1.1 | 19.8 | 56308 | 0.5477 | 1.1066 | 1.0460 | 93.57 | 88.90 | 7.65 |
| 1.1 | 19.8 | 54664 | 0.5323 | 1.0753 | | | | |
| 1.2 | 20.1 | 48242 | 0.4718 | 0.9388 | | | | |
| 1.2 | 20.1 | 54888 | 0.5344 | 1.0634 | | | | |
| 2.1 | 20.4 | 51096 | 0.4987 | 0.9778 | 0.9638 | 95.02 | | |
| 2.1 | 20.4 | 48505 | 0.4742 | 0.9299 | | | | |
| 2.2 | 21.3 | 55909 | 0.5440 | 1.0216 | | | | |
| 2.2 | 21.3 | 50498 | 0.4930 | 0.9259 | | | | |
| 3.1 | 20.9 | 36505 | 0.3612 | 0.6913 | 0.6649 | 78.10 | | |
| 3.1 | 20.9 | 36620 | 0.3623 | 0.6934 | | | | |
| 3.2 | 21.3 | 33421 | 0.3322 | 0.6238 | | | | |
| 3.2 | 21.3 | 34960 | 0.3467 | 0.6510 | | | | |

**Table 35 Stability of curcumin-NLC 9ES bead powder at 4 degrees Celsius after 1 month**

| 9ES | Weight (mg) | Peak area | Concentrations (µg /ml) | amount of Curcumin in 1 mg | avg | %Drug remaining | mean | SD |
|---|---|---|---|---|---|---|---|---|
| 1.1 | 20.3 | 51806 | 0.5053 | 0.9957 | 0.9920 | 108.25 | 97.62 | 7.53 |
| 1.1 | 20.3 | 51317 | 0.5007 | 0.9867 | | | | |
| 1.2 | 20.7 | 51312 | 0.5007 | 0.9675 | | | | |
| 1.2 | 20.7 | 54095 | 0.5269 | 1.0182 | | | | |
| 2.1 | 20 | 44952 | 0.4408 | 0.8816 | 0.9532 | 92.80 | | |
| 2.1 | 20 | 49387 | 0.4826 | 0.9651 | | | | |
| 2.2 | 19.6 | 50120 | 0.4895 | 0.9989 | | | | |
| 2.2 | 19.6 | 48470 | 0.4739 | 0.9672 | | | | |
| 3.1 | 20.7 | 44030 | 0.4321 | 0.8350 | 0.9052 | 91.81 | | |
| 3.1 | 20.7 | 48369 | 0.4730 | 0.9139 | | | | |
| 3.2 | 22 | 53070 | 0.5172 | 0.9404 | | | | |
| 3.2 | 22 | 52554 | 0.5124 | 0.9316 | | | | |

**Table 36 Stability of curcumin-NLC 9ES bead powder at room temperature after 3 months**

| 9ES | Weight (mg) | Peak area | Concentrations (µg /ml) | amount of Curcumin in 1 mg | avg | %Drug remaining | mean | SD |
|---|---|---|---|---|---|---|---|---|
| 1.1 | 21.4 | 47437 | 0.4642 | 0.8676 | 0.8224 | 73.56 | | |
| 1.1 | 21.4 | 46712 | 0.4574 | 0.8549 | | | | |
| 1.2 | 19.9 | 40111 | 0.3952 | 0.7943 | | | | |
| 1.2 | 19.9 | 38964 | 0.3844 | 0.7726 | | | | |
| 2.1 | 19.7 | 42860 | 0.4211 | 0.8550 | 0.8336 | 82.18 | | |
| 2.1 | 19.7 | 43440 | 0.4265 | 0.8661 | | | | |
| 2.2 | 19.5 | 40007 | 0.3942 | 0.8086 | | | 72.69 | 8.13 |
| 2.2 | 19.5 | 39795 | 0.3922 | 0.8045 | | | | |
| 3.1 | 21.1 | 28513 | 0.2859 | 0.5421 | 0.5305 | 62.32 | | |
| 3.1 | 21.1 | 27504 | 0.2764 | 0.5241 | | | | |
| 3.2 | 20.6 | 27201 | 0.2736 | 0.5312 | | | | |
| 3.2 | 20.6 | 26841 | 0.2702 | 0.5246 | | | | |

**Table 37 Stability of curcumin-NLC 9ES bead powder at 4 degrees Celsius after 3 months**

| 9ES | Weight (mg) | Peak area | Concentrations (µg /ml) | amount of Curcumin in 1 mg | avg | %Drug remaining | mean | SD |
|---|---|---|---|---|---|---|---|---|
| 1.1 | 21.6 | 56565 | 0.5502 | 1.0188 | 0.9508 | 103.76 | | |
| 1.1 | 21.6 | 60311 | 0.5854 | 1.0842 | | | | |
| 1.2 | 22.7 | 49544 | 0.4840 | 0.8529 | | | | |
| 1.2 | 22.7 | 49214 | 0.4809 | 0.8474 | | | | |
| 2.1 | 20.3 | 47682 | 0.4665 | 0.9192 | 0.9535 | 92.83 | | |
| 2.1 | 20.3 | 47391 | 0.4638 | 0.9138 | | | | |
| 2.2 | 19.9 | 51408 | 0.5016 | 1.0082 | | | 94.54 | 6.94 |
| 2.2 | 19.9 | 49543 | 0.4840 | 0.9729 | | | | |
| 3.1 | 20.6 | 44164 | 0.4334 | 0.8415 | 0.8581 | 87.02 | | |
| 3.1 | 20.6 | 45193 | 0.4431 | 0.8603 | | | | |
| 3.2 | 21 | 44847 | 0.4398 | 0.8377 | | | | |
| 3.2 | 21 | 47920 | 0.4687 | 0.8928 | | | | |

**Table 38 Stability of curcumin-NLC 9ES bead powder at room temperature after 6 months**

| 9ES | Weight (mg) | Peak area | Concentrations (µg /ml) | amount of Curcumin in 1 mg | avg | %Drug remaining | mean | SD |
|---|---|---|---|---|---|---|---|---|
| 1.1 | 20.6 | 30189 | 0.3017 | 0.5859 | 0.7038 | 62.95 | 65.88 | 7.26 |
| 1.1 | 20.6 | 35794 | 0.3545 | 0.6884 | | | | |
| 1.2 | 20.1 | 38459 | 0.3796 | 0.7555 | | | | |
| 1.2 | 20.1 | 40053 | 0.3946 | 0.7854 | | | | |
| 2.1 | 20.2 | 43855 | 0.4304 | 0.8524 | 0.7696 | 75.87 | | |
| 2.1 | 20.2 | 38387 | 0.3789 | 0.7504 | | | | |
| 2.2 | 19.6 | 36745 | 0.3635 | 0.7418 | | | | |
| 2.2 | 19.6 | 36323 | 0.3595 | 0.7337 | | | | |
| 3.1 | 20.2 | 25181 | 0.2546 | 0.5041 | 0.5007 | 58.82 | | |
| 3.1 | 20.2 | 22915 | 0.2332 | 0.4618 | | | | |
| 3.2 | 20.8 | 25831 | 0.2607 | 0.5013 | | | | |
| 3.2 | 20.8 | 27733 | 0.2786 | 0.5358 | | | | |

**Table 39 Stability of curcumin-NLC 9ES bead powder at 4 degrees Celsius after 6 months**

| 9ES | Weight (mg) | Peak area | Concentrations (µg /ml) | amount of Curcumin in 1 mg | avg | %Drug remaining | mean | SD |
|---|---|---|---|---|---|---|---|---|
| 1.1 | 21.2 | 52836 | 0.5150 | 0.9718 | 0.9681 | 105.64 | 92.55 | 9.72 |
| 1.1 | 21.2 | 55399 | 0.5392 | 1.0173 | | | | |
| 1.2 | 20.7 | 48603 | 0.4752 | 0.9182 | | | | |
| 1.2 | 20.7 | 51176 | 0.4994 | 0.9650 | | | | |
| 2.1 | 20.7 | 48909 | 0.4781 | 0.9238 | 0.9203 | 89.60 | | |
| 2.1 | 20.7 | 46858 | 0.4587 | 0.8864 | | | | |
| 2.2 | 21.1 | 51231 | 0.4999 | 0.9477 | | | | |
| 2.2 | 21.1 | 49866 | 0.4871 | 0.9234 | | | | |
| 3.1 | 20.8 | 41082 | 0.4043 | 0.7776 | 0.8125 | 82.40 | | |
| 3.1 | 20.8 | 42683 | 0.4194 | 0.8066 | | | | |
| 3.2 | 19.9 | 43076 | 0.4231 | 0.8505 | | | | |
| 3.2 | 19.9 | 41214 | 0.4056 | 0.8152 | | | | |

**X-ray diffraction (XRD) and Fourier transformation infrared spectroscopy (FTIR)**

The structural analysis of lyophilized blank NLCs (B-NLCs), curcumin-NLCs (C-NLCs), blank ES100 beads (7ESB and 9ESB), and curcumin-NLC beads (7ESC and 9ESC) were recorded using a Fourier Transform Infrared (FTIR) Spectroscopy (Perkin Elmer model Spectrum GX, USA) in a range from 4000 to 400 $cm^{-1}$ with a resolution of 0.5 $cm^{-1}$.

The crystalline structure of lyophilized blank NLCs (B-NLCs), curcumin-NLCs (C-NLCs), blank ES100 beads (7ESB and 9ESB), and curcumin-NLC beads (7ESC and 9ESC) were measured at room temperature in the range from 5 to 50° with Cu Kα radiation (λ = 0.154 nm, 30 kV, 10 mA), the process parameters were set as: scan step size of 0.02°, scan step time of 0.05 s by X-ray diffraction (XRD; D2 Phaser, Bruker, USA).

**Result**

The physicochemical characterizations of the curcumin-NLCs (7ES, 9ES) have been done by XRD and FTIR, as shown below. However, the result showed no difference between these 2 formulations. The results also showed no difference between formulation and its blank. (Figure.30)

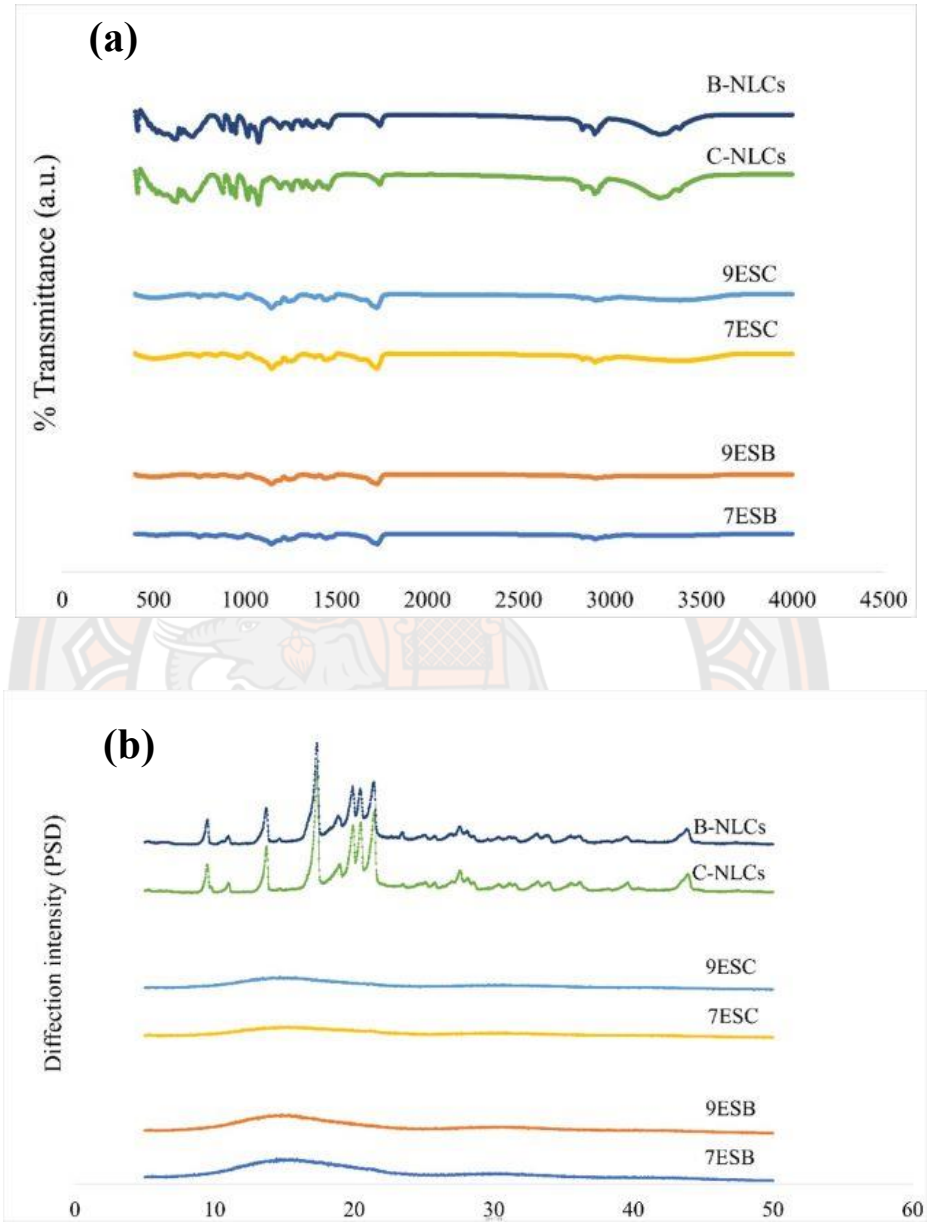


**Figure 30 FTIR spectrum (a), and XRD patterns (b) of lyophilized blank NLCs (B-NLCs), curcumin-NLCs (C-NLCs), blank ES100 beads (7ESB and 9ESB), and curcumin-NLC beads (7ESC and 9ESC)**

**Table 40 Estimated parameters obtained from fitting experimental data of curcumin-NLCS beads to different kinetic models**

| **7ES** | | | | | |
|---|---|---|---|---|---|
| **Parameter** | **Zero-order** | **First-order** | **Higuchi** | **Korsmeyer** | **Hopfenberg** |
| N_observed | 6 | 6 | 6 | 6 | 6 |
| R_obs-pre | 0.9612 | 0.9450 | 0.9362 | 0.9802 | 0.9944 |
| Rsqr | 0.9239 | 0.8926 | 0.8765 | 0.9592 | 0.9889 |
| Rsqr_adj | 0.9049 | 0.8658 | 0.8457 | 0.9320 | 0.9815 |
| MSE | 36.4763 | 51.4476 | 59.1601 | 26.0559 | 7.0903 |
| MSE_root | 6.0396 | 7.1727 | 7.6916 | 5.1045 | 2.6628 |
| SS | 145.9052 | 205.7906 | 236.6403 | 78.1677 | 21.2710 |
| WSS | 145.9052 | 205.7906 | 236.6403 | 78.1677 | 21.2710 |
| AIC | 33.8977 | 35.9612 | 36.7992 | 32.1531 | 24.3441 |
| MSC | 1.5809 | 1.2370 | 1.0973 | 1.8717 | 3.1732 |
| **9ES** | | | | | |
| **Parameter** | **Zero-order** | **First-order** | **Higuchi** | **Korsmeyer** | **Hopfenberg** |
| N_observed | 6 | 6 | 6 | 6 | 6 |
| R_obs-pre | 0.9851 | 0.9747 | 0.9723 | 0.9832 | 0.9863 |
| Rsqr | 0.9704 | 0.9497 | 0.9453 | 0.9647 | 0.9727 |
| Rsqr_adj | 0.9630 | 0.9371 | 0.9316 | 0.9411 | 0.9545 |
| MSE | 12.4404 | 21.1238 | 22.9775 | 19.7891 | 15.2847 |
| MSE_root | 3.5271 | 4.5961 | 4.7935 | 4.4485 | 3.9096 |
| SS | 49.7615 | 84.4951 | 91.9099 | 59.3672 | 45.8540 |
| WSS | 49.7615 | 84.4951 | 91.9099 | 59.3672 | 45.8540 |
| AIC | 27.4435 | 30.6202 | 31.1249 | 30.5025 | 28.9528 |
| MSC | 2.3532 | 1.8238 | 1.7397 | 1.8434 | 2.1017 |

# BIOGRAPHY

**Name-Surname** Jittakan Lertpairod

**Date of Birth**

**Address**

**Education Background** 2017 Pharm.D. (Pharm. Care), Naresuan University

**Publication** Lertpairod, J., Tiyaboonchai, W. pH-sensitive beads containing curcumin loaded nanostructured lipid carriers for a colon targeted oral delivery system. J. Pharm. Investig. 52, 387–396 (2022). https://doi.org/10.1007/s40005-022-00572-0